Mon. Not. R. Astron. Soc. **000**, 1–16 (2012) Printed 2 July 2012 (MN LaTeX style file v2.2)

Spectroscopic follow-up of UV-excess objects selected from the UVEX survey

Kars Verbeek[1⋆], Paul J. Groot[1], Simone Scaringi[1], Ralf Napiwotzki[2], Ben Spikings[2], Roy H. Østensen[3], Janet Drew[2], Danny Steeghs[4], Jorge Casares[5], Jesus M. Corral-Santana[5,6] Romano Corradi[5,7], Niall Deacon[8] Jeremy Drake[9] Boris T. Gänsicke[4], Eduardo González-Solares[10], Robert Greimel[11], Ulrich Heber[12], Mike Irwin[10], Christian Knigge[13] and Gijs Nelemans[1]

[1] *Department of Astrophysics, Radboud University Nijmegen, P.O. Box 9010, 6500 GL Nijmegen, The Netherlands*
[2] *Centre for Astronomy Research, Science & Technology Research Institute, University of Hertfordshire, Hatfield, AL10 9AB, UK*
[3] *Instituut voor Sterrenkunde, KU Leuven, Celestijnenlaan 200D, B-3001 Leuven, Belgium*
[4] *Physics Department, University of Warwick, Coventry, CV4 7AL, UK*
[5] *Instituto de Astrofísica de Canarias, Via Lactea, s/n E-38205 La Laguna (Tenerife), Spain*
[6] *Departamento de Astrofísica, Universidad de La Laguna, La Laguna E-38205, S/C de Tenerife, Spain*
[7] *Isaac Newton Group of Telescopes, Apartado de Correos 321, E-38700 Santa Cruz de La Palma, Canary Islands, Spain*
[8] *Institute for Astronomy, University of Hawaii, 2680 Woodlawn Drive, Honolulu, HI 96822, USA*
[9] *Harvard Smithsonian CfA, HCO/SAO, MS 3, 60 Garden Str, US Cambridge MA 02138-1516, United States*
[10] *Cambridge Astronomy Survey Unit, Institute of Astronomy, University of Cambridge, Madingley Road, Cambridge, CB3 0HA, UK*
[11] *Institut für Physik, Karl-Franzen Universität Graz, Universitätsplatz 5, 8010 Graz, Austria*
[12] *Dr. Remeis-Sternwarte Bamberg, Universität Erlangen-Nürnberg, Sternwartstrasse 7, D-96049 Bamberg, Germany*
[13] *School of Physics and Astronomy, University of Southampton, Southampton, Hampshire, SO17 1BJ, UK*

Accepted ... Received ...; in original form ...

ABSTRACT

We present the results of the first spectroscopic follow-up of 132 optically blue UV-excess sources selected from the UV-excess survey of the Northern Galactic Plane (*UVEX*). The UV-excess spectra are classified into different populations and grids of model spectra are fit to determine spectral types, temperatures, surface gravities and reddening. From this initial spectroscopic follow-up 95% of the UV-excess candidates turn out to be genuine UV-excess sources such as white dwarfs, white dwarf binaries, subdwarfs type O and B, emission line stars and QSOs. The remaining sources are classified as slightly reddened main-sequence stars with spectral types later than A0V. The fraction of DA white dwarfs is 47% with reddening smaller than $E(B-V)\leqslant 0.7$ mag. Relations between the different populations and their *UVEX* photometry, Galactic latitude and reddening are shown. A larger fraction of *UVEX* white dwarfs is found at magnitudes fainter than $g>17$ and Galactic latitude smaller than $|b|<4$ compared to main-sequence stars, blue horizontal branch stars and subdwarfs.

Key words: surveys – stars:general – ISM:general – Galaxy: stellar content – Galaxy: disc – Stars: white dwarfs – Stars: subdwarfs

1 INTRODUCTION

Traditionally, surveys searching for faint blue objects have avoided the Galactic Plane because of the high dust absorption. Surveys searching for quasars and white dwarfs therefore mostly observed at Galactic latitudes larger than $|b|>30^\circ$. Examples of such surveys are the Palomar Green survey (PG, Green et al., 1986), the Kiso survey (Wegner et al., 1987, Limoges et al., 2010), the Sloan Digital Sky survey (SDSS, York et al., 2000, Yanni et al., 2009 and Eisenstein et al., 2006) and the Hamburg Quasar survey (HQS, Hagen et al., 1995, Homeier et al., 1998) in the northern hemisphere and the Montreal-Cambridge-Tololo survey (MCT, Lamontagne et al., 2000, Demers 1986), the Edinburgh-Cape survey (EC, Kilkenny et al., 1997, Stobie et al., 1997), the Homogeneous Bright Quasar survey (Gemmo et al., 1995) and the Hamburg-ESO survey (Christlieb et al., 2001, Wisotzki et al., 1996) in the southern hemisphere.

⋆ E-mail:k.verbeek@astro.ru.nl

Only the Kitt Peak-Downes survey (KPD, Downes et al., 1986) survey and the Sandage Two-colour Galactic Plane survey (Lanning, 1973) observed a bit closer to the Galactic Plane. Some of the brighest *UVEX* UV-excess sources are Lanning sources (e.g. UVEXJ0328+5035 and UVEXJ0528+2716 in Table AA1 are in Lanning, 1973 and Lanning et al., 2004 respectively). The lowest Galactic latitudes $|b| < 5°$ are still relatively unexplored (see e.g. Fig.2 of Napiwotzki et al., 2003). In order to determine key population characteristics of Galactic sources, such as their scaleheight or space density, it is crucial to study the low Galactic latitude environment. The space density of stellar remnants, such as white dwarfs, Cataclysmic Variables and AM CVn stars, is currently poorly constrained while there must be $\sim 10^5$ of them in the Milky Way (see Fig. 1 of Groot et al., 2009, McCook et al., 1999, Lépine et al., 2011 and Nelemans et al., 2001).

One of the main goals of the European Galactic Plane Surveys (*EGAPS*) is to obtain a homogeneous sample of evolved objects in our Milky Way with well-known selection limits. The UV-excess survey of the Northern Galactic Plane (*UVEX* , Groot et al., 2009) images a 10×185 degrees wide band (–5°< b <+5°) centred on the Galactic equator in the U, g, r and He I λ5875 bands down to $\sim 21^{st} - 22^{nd}$ magnitude using the Wide Field Camera mounted on the Isaac Newton Telescope on La Palma. From the first 211 square degrees of *UVEX* data, a catalogue of 2 170 optically blue UV-excess candidates was selected in Verbeek et al. (2012; hereafter V12). These UV-excess sources were selected from the $(U - g)$ versus $(g - r)$ colour-colour diagram and g versus $(U - g)$ and g versus $(g - r)$ colour-magnitude diagrams by an automated field-to-field selection algorithm. This automated selection algorithm and the properties of the selected UV-excess catalogue are described in V12. Less than ∼1% of the selected UV-excess sources are currently known in the literature.

Here we report our spectroscopic follow-up for 132 objects (6%) in the UV-excess catalogue of V12. This early reconnaissance is important for the design of future colour-selection methods for various populations, comparable to the selection techniques for e.g. the SDSS, which generally do not have to deal with the added complication of reddening (Gänsicke et al., 2009, Girven et al., 2011). In Sect. 2 the spectroscopy of the selected sample is described, and in Sect. 3 the spectra are presented and classified. The spectra are fitted to grids of model spectra in order to determine the characteristics of UV-excess spectra classified as white dwarfs, subdwarfs, main-sequence stars and blue horizontal branch stars. Finally in Sect. 4 we summarise the conclusions of the UV-excess catalogue and the spectroscopic follow-up. The UV-excess spectra are shown in Figs. A1 to A11 and their features are listed in Table AA1 in Appendix A. All spectra and the table can also be obtained from the *UVEX* website[1].

[1] http://www.uvexsurvey.org

2 SPECTROSCOPIC FOLLOW-UP OF UV-EXCESS CANDIDATES

Spectroscopic follow-up was obtained by three different telescopes for a total of 132 UV-excess candidates during a number of observing runs. For 100 UV-excess candidates spectroscopic observations were obtained, during two runs in September 2009 and December 2010, with the Intermediate dispersion Spectrograph and Imaging System (ISIS) mounted at the 4.2m William Herschel Telescope (WHT) at Roque de los Muchachos Observatory, on the island of La Palma. The blue and red arms of the spectrograph were used in combination with the standard 5300 dichroic and no order sorting filter. The gratings $R300B$ in the blue arm and $R316R$ in the red arm were used giving a dispersion of 0.86 Å/pix and 0.93 Å/pix, respectively. The central wavelengths of the blue and red arms were λ_c=4 700 Å and λ_c=6 650 Å, respectively. The slit width (1.2-1.5 arcsec) was matched with the seeing during the observations: typically 20-30 percent larger than the seeing. The binning was 2×2 and the read-out speed slow. We used integration times from 300 seconds for the brightest objects at g∼15 to 1500 seconds for the fainter sources at g∼20. This gives signal-to-noise ratio SNR⩾20, which is required for spectroscopic identification of the UV-excess sources. The goal was to obtain a sample of spectra, distributed equally over g magnitude and $(g - r)$ colours in the magnitude range $13 < g < 20$, covering the entire g vs. $(g - r)$ colour-magnitude diagram. Due to the weather and the location of the Galactic Plane during the observations the sample is biased in magnitude and right ascension. For statistics it is important to be aware of this bias.

All the WHT/ISIS spectra were reduced using IRAF[2]. Bias and flat field corrections, trimming and extraction of the spectra were done in the standard way. The spectra were wavelength calibrated using CuNe+CuAr calibration arcs. Standard stars BD+28°4211, BD+25°4655, G191–B2B, Feige 34 and Feige 110 were used for the flux calibration of the spectra. The spectra were not corrected for telluric absorption. Effects of cosmic rays not removed by IRAF were corrected by hand by interpolating these pixels to the average flux of the neighbouring pixels. The reduced WHT/ISIS spectra cover the wavelength range λ=3 700 Å to λ=8 100 Å, with a dichroic gap from λ=5 200–5 600 Å. Two additional WHT/ISIS spectra with similar characteristics were obtained during a run in October 2008 during follow-up of IPHAS-POSS high proper motion candidates (Deacon et al., 2009).

Furthermore, twenty-six Hectospec (Fabricant et al., 2004) spectra are available for the UV-excess candidates. These 26 spectra were obtained with the MMT+Hectospec combination during *IPHAS* follow-up observations between 2004 and 2007, described in Sect 2.1 of Vink et al. (2008). Hectospec is a multi-object spectrograph, fed by 300

[2] Image Reduction and Analysis Facility (IRAF) is distributed by the National Optical Astronomy Observatory, which is operated by the Association of Universities for Research in Astronomy (AURA) under cooperative agreement with the National Science Foundation.

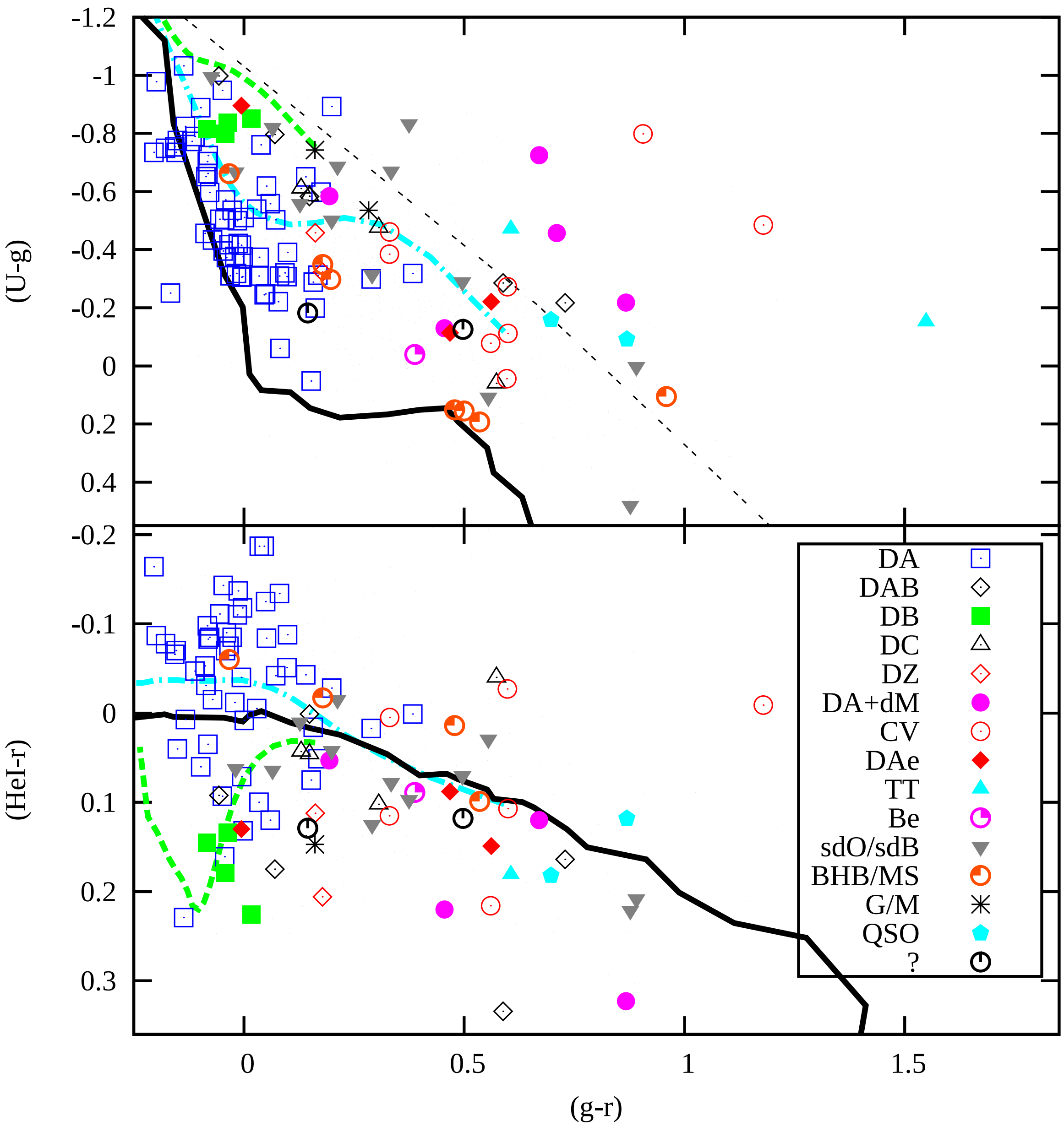

Figure 1. The UVEX colour-colour diagrams with the classified UV-excess candidates. The lines are the simulated colours of unreddened main-sequence stars (solid black) and the O5V-reddening line (dashed black) of V12. The cyan and green dashed lines are respectively the simulated colours of unreddened Koester DA and DB white dwarfs. The different symbols indicate the classification: White Dwarf (DA/DB/DAB/DC/DZ/DAe), White Dwarf+Red Dwarf binary (DA+dM), Cataclysmic Variable (CV), T Tauri star (TT), Be star (Be), subdwarf star (sdO/sdB), main-sequence star or blue horizontal branch star (MS/BHB), G2V star and M-giant (G/M), Quasi Stellar Object (QSO) and unknown (?). The sources classified as "noisy" in Sect. 3.2 are not shown here. There is one more Hα emitter classified as T Tauri star at $(g-r)$=1.55, $(HeI-r)$=0.6 and one M-giant at $(g-r)$=0.28, $(HeI-r)$=–1.9 not shown in the $(HeI-r)$ vs. $(g-r)$ colour-colour diagram.

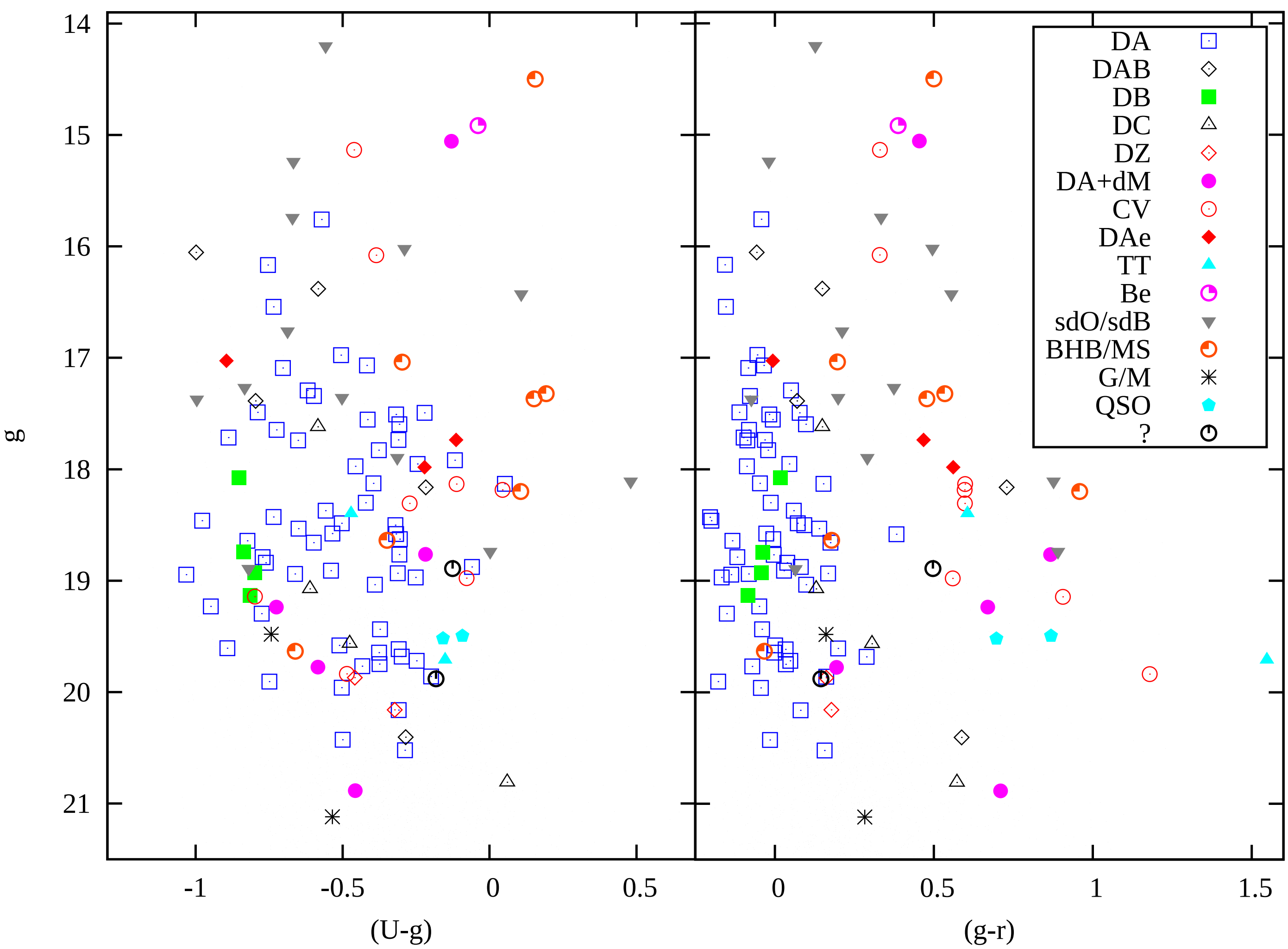

Figure 2. The UVEX colour-magnitude diagrams with the classified UV-excess candidates.

robotically-positioned optical fibers, attached to the 6.5m MMT telescope on Mount Hopkins, Arizona, USA. The spectra cover the wavelength range λ=4 000–8 500 Å and have a dispersion of ∼6 Å/pix. Of the 26 Hectospec spectra 5 spectra are flux calibrated. The extracted Hectospec were corrected for incomplete sky subtraction (Vink et al., 2008) and background sky spectra were checked in order to confirm the emission lines. Some of the Hectospec spectra shown in Appendix A still show emission features at the wavelengths of the Balmer lines due to bad sky subtraction in fields with diffuse emission (Fabricant et al., 2005).

Additionally, the FAST spectrograph (Fabricant et al., 1998), mounted on the 60-inch Tillinghast telescope, located at the Fred Lawrence Whipple Observatory (FLWO) on Mount Hopkins, Arizona, obtained spectra for candidates in the *IPHAS* Hα emission line list (Witham et al., 2008) and candidates in the catalogues of V12. There are 4 FAST spectra for our UV-excess candidates obtained between 2009 and 2012. The FAST spectra cover the wavelength range λ=3 800–7 400 Å with a dispersion of ∼3 Å/pix.

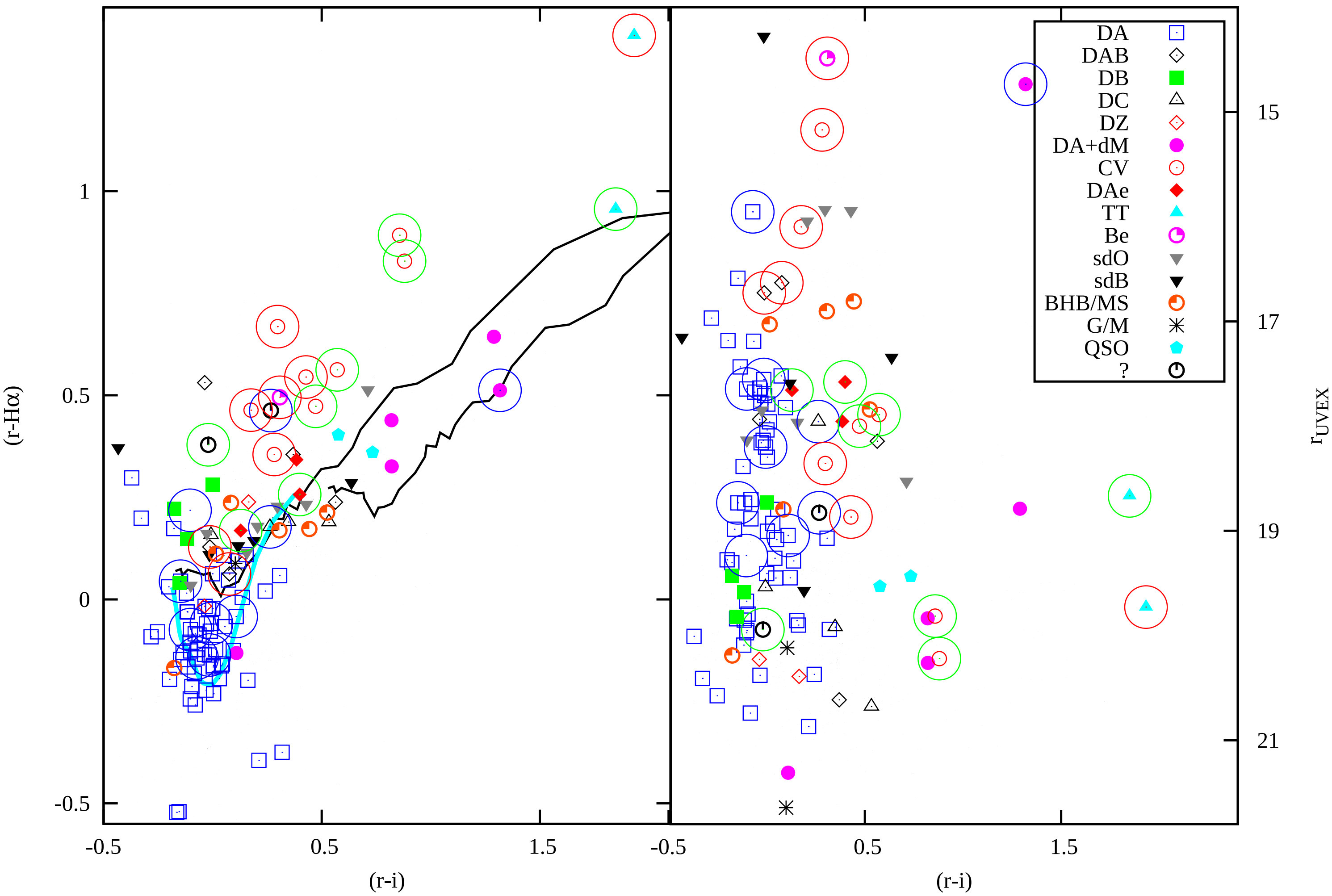

Figure 3. IPHAS colour-colour and colour-magnitude diagrams with the classified UV-excess candidates that have a match in IPHAS. There is one extra sources classified as M-giant at $(r-i)$=0.1, $(r-H\alpha)$=2.25 in the $(r-H\alpha)$ vs. $(r-i)$ colour-colour diagram. The lines are the synthetic colours of main-sequence stars (black) with reddening $E(B-V)$=0 and $E(B-V)$=1 and unreddened Koester DA white dwarfs (cyan). Sources that are in the Deacon IPHAS-POSSI PM catalogue are encircled blue, sources that are in the Witham Hα emission line catalogue are encircled red and sources that show Hα emission lines in their spectra but are not in the Witham catalogue are encircled green. The Witham catalogue covers the magnitude range 13< r <19.5 and the Deacon catalogue covers the magnitude range 13.5< r <19. The sources classified as "noisy" in Sect. 3.2 are not shown here, one of them has a match in the IPHAS-POSSI PM catalogue.

3 THE CLASSIFICATION OF THE SPECTROSCOPIC OBSERVATIONS

The results of the spectroscopic observations are presented in Table AA1 in Appendix A, ordered by RA. The spectra of all UV-excess sources are shown in Figs. A1 to A11 in Appendix A. An overview of the classification is summarized in Table 1 and the classified sources are plotted in the colour-colour and colour-magnitude diagrams of Figs. 1 to 3. The INT/WFC Photometric Hα Survey of the Northern Galactic Plane (*IPHAS* , Drew et al., 2005) imaged the same survey area as *UVEX* in the r, i and $H\alpha$ filters, the *IPHAS* IDR data (González-Solares et al., 2008) are used in Fig. 3. In the *IPHAS* colour-colour and colour-magnitude diagram sources with a match in Witham Hα emission line catalogue (Witham et al., 2008) or IPHAS-POSS proper motion catalogue (Deacon et al., 2009) are encircled red

Table 1. Classification of UV-excess spectra.

Spec.Type	Number	Fraction (%)
DA	62	46.6
DB	4	3.0
DAB/DBA	5	3.8
DC	4	3.0
DZ	2	1.5
DA+dM	5	3.8
DAe	3	2.3
CV	8	6.0
T Tauri	2	1.5
Be	1	0.8
sdO	7	5.3
sdB	6	4.5
BHB/MS/F	4	3.0
BHB/MS/B	3	2.3
G/M	2	1.5
QSO	2	1.5
Unknown	2	1.5
Noisy	10	7.6

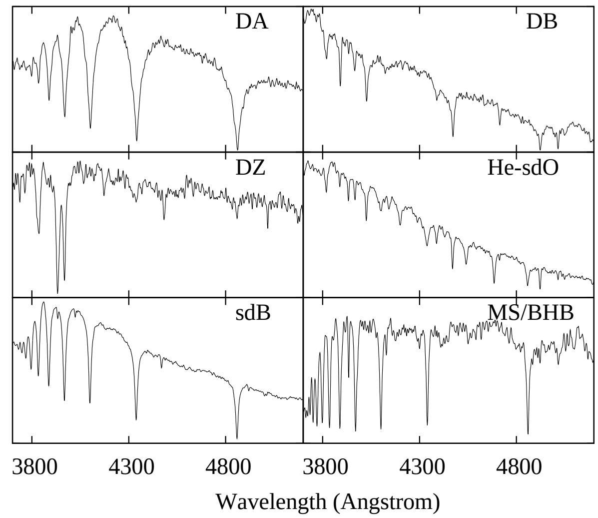

Figure 4. Example of 6 UV-excess spectra: DA white dwarf (UVEXJ0113+5819), DB white dwarf (UVEXJ0002+6236), DZ white dwarf (UVEXJ0418+4417), He-sdO (UVEXJ0221+5648), sdB (UVEXJ0202+5643) and MS/BHB star (UVEXJ0228+5846).

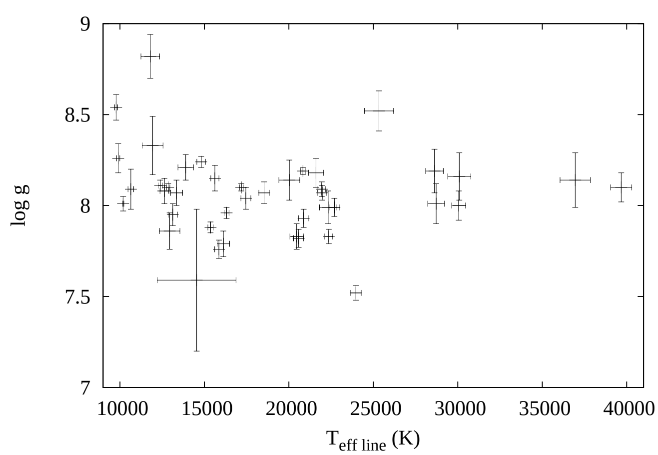

Figure 5. Temperature-gravity diagram of the UV-excess hydrogen atmosphere white dwarfs, determined through line profile fitting.

and blue respectively. Note that a global photometric calibration is not applied to the *UVEX* data yet, so the magnitudes and colours of the UV-excess sources might show a small scatter (similar to the early *IPHAS* data, e.g. Drew et al., 2005). Additionally, there is a likely systematic shift in $(U-g)$ of 0.2-0.3 magnitudes for all sources. This U-band shift in the INT/WFC data was already reported in Greiss et al. (2012). Both effects do not influence the result of the selection method and the content of the UV-excess catalogue because the selection was done relative to the reddened main-sequence population (see V12 for details), however the shift does apply to the $(U-g)$ colours given in Table AA1.

3.1 The UV-excess spectra classified as white dwarfs

A first classification of the UV-excess spectra is done by comparing them with model spectra by eye. White dwarfs and emission-line star spectra are separated from the subdwarf type O and B, main-sequence and blue horizontal branch star spectra (see Sect. 3.2). Hydrogen atmosphere (DA) white dwarfs are easily recognizable by their broad Balmer lines. We use the classification criteria of Sion et al. (1983) and the atlas of Wesemael et al. (1993) to classify the other different types of white dwarfs by eye. In total we classify 85 spectra as white dwarfs. Sixty-two show only Balmer lines (DA), there are 4 white dwarfs showing only HeI lines (DB) and 5 white dwarfs showing both Balmer and HeI lines (DBA/DAB). Four white dwarfs have a continuum spectrum with no lines (DC) and 2 white dwarfs show a spectrum with strong calcium lines only but no, or only little, hydrogen and helium lines (DZ/DZA). Five objects are DA+dM composite objects, showing a DA white dwarf in the blue part of the spectrum and an M-dwarf in the red part of the spectrum (Lanning, 1982). Furthermore, there are 3 sources showing a DA white dwarf spectrum, with emission lines at the centre of their Balmer absorption lines. These DAe sources are discussed in Sect. 3.3. Example spectra of a DA white dwarf, DB white dwarf and a DZ white dwarf are shown in Fig. 4.

White dwarf model spectra are fitted to determine the effective temperature ($T_{\rm eff}$) and surface gravity ($log\,g$) of the DA white dwarfs by two independent methods. The first method, described in Napiwotzki (1997) and Napiwotzki et al. (1999), normalizes the continuum of the white dwarf spectra and then fits the absorption lines using an interpolated grid of model spectra with different $T_{\rm eff}$ and $log\,g$ at $\Delta T_{\rm eff}$=500–2 000 K and $\Delta log\,g$=0.2/0.5 intervals. The second method fits a grid of reddened white dwarfs model spectra (Koester et al., 2001) with $log\,g$=8.0 to the spectra in the range $0.0 \leqslant E(B-V) \leqslant 1.0$

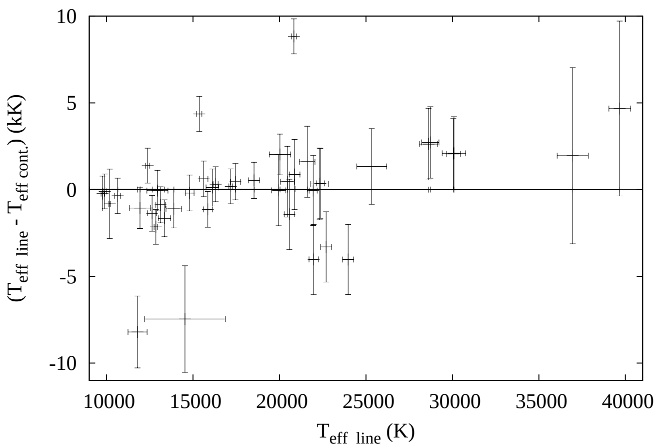

Figure 6. Comparison of the hydrogen white dwarf temperatures found by the two independent fitting methods: Method 1 fits the absorption lines of the normalized spectra and method 2 fits the continuum of the spectra including reddening.

at $\Delta E(B-V)$=0.1 intervals, using the reddening laws of Cardelli, Clayton & Mathis (1989). The second method fits the effective temperature and reddening of the white dwarfs with an accuracy of $T_{\rm eff}$∼1 000K and $E(B-V)$∼0.1 (see Sect. 4). The Hectospec white dwarf spectra are not fitted since they are not flux calibrated. The white dwarf fitting results of the two methods are listed in Table 2. The result of the first white dwarf fitting method is shown in the temperature-gravity diagram of Fig. 5, The difference between the two methods is shown in Fig. 6, where typically the results agree within the errors. Four systems do not have consistent fits, for these spectra the continuum fit of the second method seems by eye to be the most suitable. For fitting of normalised profiles there is a strong degeneracy between a "hot" and "cold" solution, due to a similar equivalent width of the Balmer lines, here the second method is more robust regarding the temperature since the slope is taken into account. The object IDs from Table 2 are overplotted in the colour-colour diagrams of Fig. 7. The reddenings found by the second fitting method are shown in the histogram of Fig. 8. Hydrogen white dwarfs typically show a reddening of $0.0 \leqslant E(B-V) \leqslant 0.1$ with a reddening up to $E(B-V) \leqslant 0.7$ for the hotter white dwarfs. As expected given their intrinsic luminosities, we see hot white dwarfs out to larger distances compared to cool white dwarfs, thus hot white dwarfs typically suffers from slightly larger reddening compared to cooler white dwarfs. Cool white dwarfs can only have little reddening since they are an intrinsically faint local population.

3.2 The UV-excess spectra classified as hot subdwarfs, MS stars and BHB stars

For the classification of hot subdwarfs, main-sequence stars (MS) and blue horizontal branch stars (BHB) stars we follow the classification scheme as outlined in Fig.1 of Moehler et al. (1990). Most sources have hydrogen and helium absorption lines clearly stronger than the hydrogen

Table 2. Result of the two fitting methods for WHT/ISIS UV-excess spectra classified as white dwarfs. The first method fits $T_{\rm eff}$ and $log\, g$, the second method fits $T_{\rm eff}$ and $E(B-V)$.

ID	UVEX name	$T_{\rm eff}$(K)/$log\, g$	$T_{\rm eff}$(K)/$E(B-V)$
1	011311.87+581902.3		10 000/0.0
2	011754.90+581815.4	11 933±619 /8.33±0.16	13 000/0.0
3	012015.68+584318.2	36 955±899 /8.14±0.15	35 000/0.2
4	012219.81+611229.9	12 801±132 /8.1 ±0.03	11 000/0.2
5	012359.82+672223.1		57 000/0.7
6	020201.82+564744.8		65 000/0.3
7	022135.47+564436.6	10 183±46 /8.01±0.04	22 000/0.2
8	022151.40+563815.7	28 621±522 /8.19±0.12	26 000/0.1
9	022510.84+580156.6	13 124±274 /7.95±0.06	14 000/0.0
10	022615.13+581710.2	9 772 ±90 /8.54±0.07	10 000/0.0
11	023044.92+563622.6	30 091±682 /8.16±0.13	28 000/0.1
12	032737.64+530231.1	18 531±306 /8.07±0.06	18 000/0.1
13	032807.05+525737.2	23 971±310 /7.84±0.04	28 000/0.3
14	032908.01+524400.6	22 358±235 /7.83±0.04	22 000/0.2
15	032910.60+524426.3	12 852±102 /8.10±0.02	15 000/0.0
16	033118.06+530351.3	17 185±112 /8.10±0.02	17 000/0.0
17	041045.70+461137.1	14 537±2333 /7.59±0.39	22 000/0.0
18	041053.99+450706.5	16 122±370 /7.79±0.07	16 000/0.1
19	041359.37+455151.2	12 381±121 /8.11±0.03	11 000/0.0
20	041733.05+452524.4	22 697±314 /7.99±0.05	26 000/0.2
21	041902.55+434307.1	17 454±293 /8.04±0.06	17 000/0.1
22	042110.67+440945.6	20 574±300 /7.82±0.05	22 000/0.4
23	052825.82+320859.5	9 894 ±94 /8.26±0.08	10 000/0.0
24	052847.75+322330.3	12 942±607 /7.86±0.10	13 000/0.0
25	190812.07+164029.2		17 000/0.0
26	202249.99+412423.1	15 620±240 /8.15±0.07	15 000/0.4
27	202255.55+412504.9	16 309±146 /7.96±0.03	16 000/0.0
28	202350.92+423826.0	25 335±864 /8.52±0.11	24 000/0.1
29	202439.91+400630.7		24 000/0.0
30	202457.34+410804.1		22 000/0.1
31	202501.86+411626.0	14 805±252 /8.24±0.03	15 000/0.3
32	202557.21+400949.2		30 000/0.1
33	202800.47+405620.0		20 000/0.0
34	203739.63+413216.3		17 000/0.3
35	205037.81+424618.9		17 000/0.1
36	205148.13+442408.8		26 000/0.0
37	210037.77+501029.0	20 873±308 /7.93±0.05	20 000/0.0
38	210248.44+475058.9	13 348±359 /8.07±0.07	15 000/0.0
39	211718.18+550638.7		22 000/0.0
40	212409.05+555521.4		12 000/0.0
41	212852.14+542048.4	13 891±457 /8.21±0.07	15 000/0.0
42	222940.17+610700.7	22 325±515 /7.99±0.09	22 000/0.0
43	223634.77+591907.8	28 721±497 /8.01±0.11	26 000/0.1
44	223811.54+603759.9	12 633±261 /8.08±0.07	14 000/0.0
45	224010.23+555950.6	19 957±414 /3.03±0.07	20 000/0.2
46	224610.82+611450.3	20 026±617 /8.14±0.11	18 000/0.0

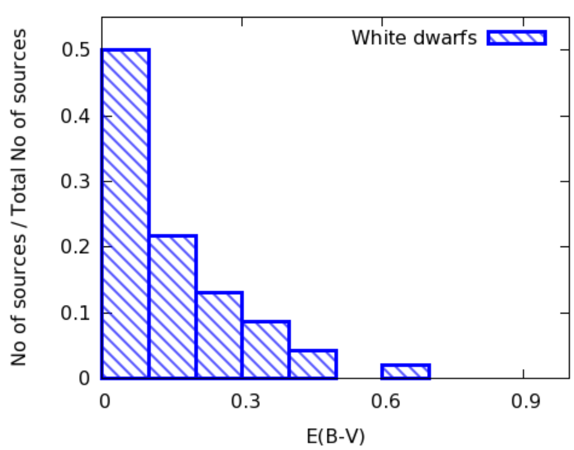

Figure 8. Distribution of $E(B-V)$ fit to the WHT/ISIS spectra of the sources classified as hydrogen atmosphere white dwarfs. The number of sources per bin is normalized by the total number of white dwarfs.

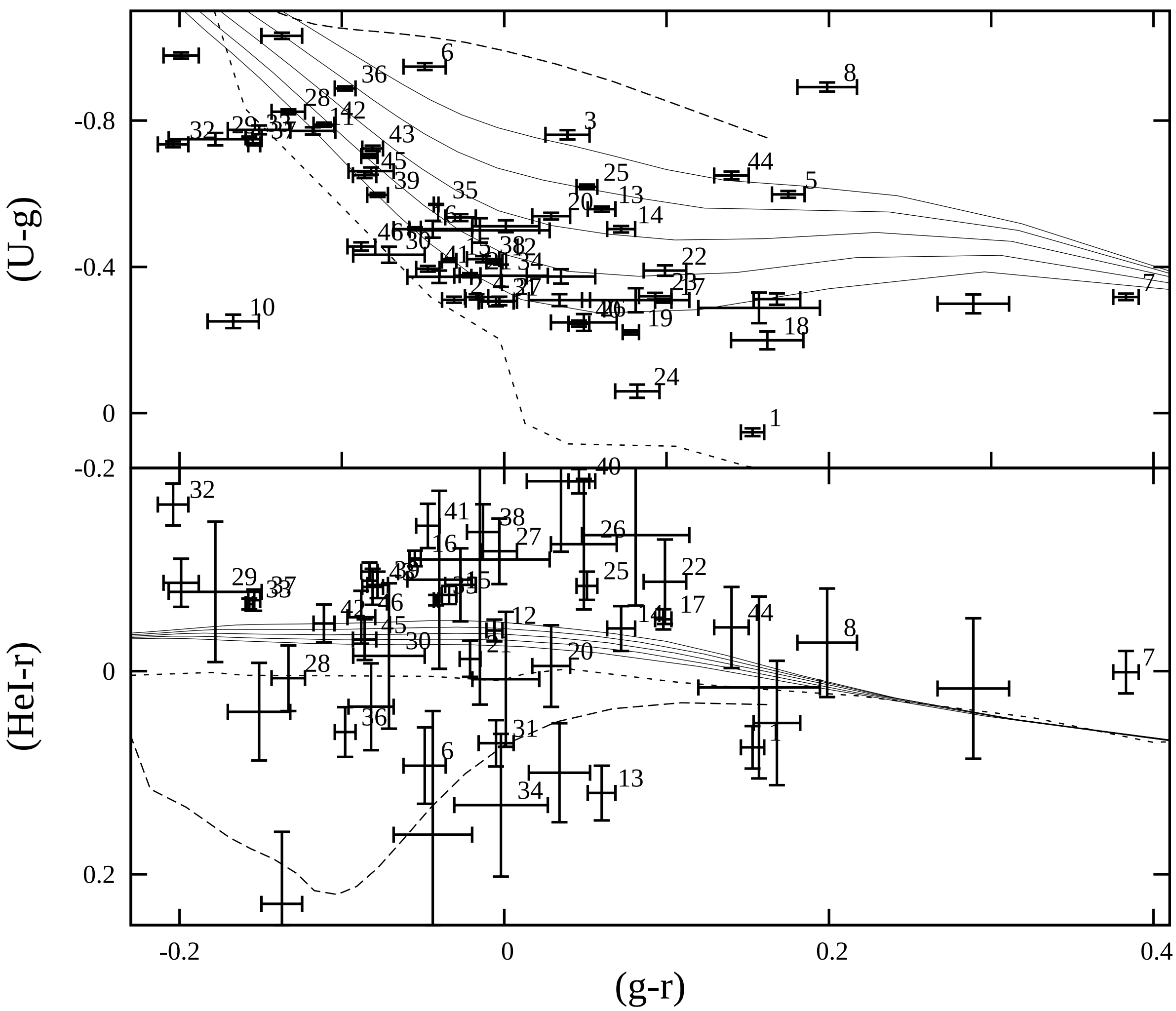

Figure 7. The UVEX colour-colour diagrams with all UV-excess sources classified as hydrogen white dwarfs, plotted with their photometric error bars. The lines are the simulated colours of unreddened main-sequence stars (dotted) and unreddened Koester DB white dwarfs (dashed) of V12 and the numbers are the white dwarf object IDs of Table 2. The five solid lines are the simulated colours of unreddened Koester DA white dwarfs with $log\,g$=7.0,7.5,8.0,8.5,9.0 (in both colour-colour diagrams the line with $log\,g$=9.0 is the most upper line). Data points and simulated colours show a likely systematic shift in $(U-g)$ colours, as explained in Greiss et al., 2012. Note that a global photometric calibration is not applied to the *UVEX* data yet, due to a scatter in the HeI-band photometry the white dwarfs do not overlap the simulated white dwarfs colours in the $(HeI-r)$ vs. $(g-r)$ colour-colour diagram. The spectra of the DA white dwarfs above or below the simulated white dwarf colours in the $(HeI-r)$ vs. $(g-r)$ colour-colour diagram do not show HeI emission or absorption.

and helium absorption lines of their best fit Pickles template spectrum, we classify these sources as hot subdwarfs (sdB/sdO). Sources with clear HeII lines are labeled sdO candidates and the sources without HeII lines are labeled sdB candidates. Grids of model spectra are fitted to the spectra of the sources classified as hot subdwarfs, MS stars and BHB stars as described in Østensen et al. (2011). The results are listed in Table 3 and the spectra of the sources classified as subdwarfs, MS stars and BHB stars are shown in Figs. A6 and A7.

From the fitting we classify 4 sources as He-sdO stars,

Table 3. Result of the fitting for UV-excess spectra classified as subdwarfs, main-sequence stars (MS) and blue horizontal branch stars (BHB). The third column shows for the He-sdO, sdO, sdB and B-type BHB/MS sources the best fit: $T_{\rm eff}$ in kK, $log\, g$ and $log\,(n(He)/n(H))$. For the MS/BHB sources without He lines the third column shows $T_{\rm eff}$ in kK and $log\, g$.

UVEX name	g	Classification/fitting
UVEXJ000016.27+603246.3	16.761	sdB (34.4/6.0/–2.8)
UVEXJ001032.27+625050.0	16.427	He-sdO
UVEXJ020201.85+564342.3	15.238	sdB (27.5/5.5/–2.8)
UVEXJ022113.52+564810.7	17.267	He-sdO (44.0/5.5/1.4)
UVEXJ022241.76+562702.2	17.895	sdB/sdO
UVEXJ022815.18+584640.8	18.200	MS/BHB (14.2/3.8)
UVEXJ031943.45+512309.0	17.368	MS/BHB (15.8/4.3)
UVEXJ032855.25+503529.8	14.202	sdB (28.5/5.5/–2.5)
UVEXJ041745.78+454049.8	17.322	MS/BHB (13.4/3.9)
UVEXJ042125.70+465115.4	18.107	sdB+F composite
UVEXJ052835.30+271650.0	14.499	BHB/MS (17.3/3.7/–1.2)
UVEXJ193809.18+305401.5	17.038	BHB/MS (18.9/4.5/–1.5)
UVEXJ193813.83+313708.1	17.373	sdO (50.4/5.7/–1.47)
UVEXJ193847.06+312024.2	19.481	G2V, $E(B-V)$=0.3
UVEXJ193951.69+302600.7	17.358	sdB (27.8/4.6/–1.5)
UVEXJ194028.01+322039.8	18.638	BHB/MS (16.0/3.1)
UVEXJ194135.69+321222.0	18.892	sdB (31.0/6.0/–1.9)
UVEXJ204210.22+443928.7	18.738	sdB/sdO
UVEXJ204957.75+401637.9	15.741	He-sdO (45.9/6.1/1.4)
UVEXJ205039.07+373958.4	21.119	M5III, $E(B-V)$=0.0
UVEXJ223941.98+585729.1	16.020	He-sdO (47.7/5.0/–0.7)
UVEXJ224521.39+551705.3	19.632	MS/BHB (14.9/4.7)

1 sdO star, 5 sdB stars, 1 sdB+F star. Two more sources are probably sdO/sdB stars but they have no accurate fitting result. The sdB+F star (UVEXJ0421+4651) has 2MASS (Cutri et al., 2003) photometry J=15.7, H=15.3, K=15.3, so the F/G star dominates in the IR completely. An example of spectra classified as He-sdO and sdB stars are shown in Fig. 4. We classify 7 sources as MS/BHB stars: 4 with $T_{\rm eff}$<16kK and 3 B-type MS/BHB stars with $T_{\rm eff}$>16kK. An example of a spectrum classified as MS/BHB star is shown in Fig. 4. Due to the signal-to-noise rate (SNR) and resolution of the spectra it is not possible to distinguish BHB stars from MS stars. Higher SNR and resolution spectra are necessary for a more reliable classification. Additionally, there is 1 G-type star and 1 M-giant in the spectroscopic sample. Ten spectra with clear hydrogen absorption lines have no fitting result. These sources are not hydrogen atmosphere white dwarfs since the Balmer lines are too narrow, they are probably subdwarfs, MS stars or BHB stars except for the source UVEXJ2036+3929, which might be a white dwarf. Since it is not possible to classify these spectra in detail and since most have low SNR they are labeled "Noisy". These spectra are shown in Fig. A11.

Template spectra of main-sequence stars and giants from the library of Pickles et al. (1998) are fit to all main-sequence and blue horizontal branch spectra, allowing for interstellar reddening in the range $0.0\leqslant E(B-V)\leqslant 1.0$ at $\Delta E(B-V)$=0.1 intervals. The accuracy of this fitting is discussed in Sect. 4. The fitting of reddened main-sequence stars including their continuum suffers from a well known degeneracy between reddened early type stars and unreddened (or less-reddened) late type stars. We use the characteristic lines of different spectral types (Morgan, Keenan & Kellman 1943) and the equivalent width of the CaII K line at λ=3 934 Å to confirm the results of the fitting method and to break degeneracies where necessary. The G-type star is a G2V star with reddening $E(B-V)$=0.3 and the M-giant has spectral type M5III with reddening $E(B-V)$=0.0. We would not expect these G2V and MIII stars in the UV-excess catalogue, they are probably selected due to the intrinsic *UVEX* photometry scatter. (see Sect. 4).

3.3 The UV-excess spectra classified as emission line stars

Among the 132 UV-excess spectra there are 11 clear Hα emission line objects, shown in in Figs. A8 to A9: 8 Cataclysmic Variables, 2 T Tauri stars and 1 Be star. We classify the Classical T Tauri from the hydrogen Balmer lines in emission on top of a M-dwarf atmosphere in combination with a U-band excess and CaII in emission (Corradi et al., 2010, Barentsen et al., 2011). The Hα emission lines of the T Tauri candidates have a width of $FWHM\sim$5 Å. The Be star is classified from the combination of a B-type continuum with Balmer absorption lines and a clear Hα emission line. Additionally, three sources show a hydrogen white dwarf spectrum, with emission cores at the centre of their Balmer absorption lines, probably indicating a close low-mass companion which is not detected in the continuum. We classify these 3 sources as DAe white dwarfs (Fig. 8 of Silvestri et al., 2006), consisting of a hot white dwarf with a very late M-dwarf companion. The *IPHAS* photometry in Fig. 3 already shows that these white dwarfs have a companion and infrared colours can be used to determine the nature of the low-mass secondaries (Verbeek et al., in prep.). An other option is that these 3 systems are Dwarf Novae (DN) (Aungwerojwit et al., 2005, Morales-Rueda & Marsh, 2002), or they might be 'pre-CV' candidates (Tappert et al., 2009 and Szkody et al., 2007). Although the hydrogen emission lines of these 3 systems is narrow, the helium emission lines are only possible when there is accretion, so they could be Cataclysmic Variables. Other objects in the UV-excess spectra are 2 Quasi Stellar Objects (QSOs), one with redshift z=2.16 at (l,b)=(125°.44, –4°.29) and one with redshift z=1.48 at (l,b)=(117°.29, –4°.43), classified using example spectra (Fig. 7 of Brunzendorf et al., 2002). For UVEXJ0110+5829 the bluest broad line in the spectrum is Lyα and the emission line at 6 030 Å is CIII. In the spectrum of UVEXJ0008+5758 the bluest line is CIV, the second line is CIII and the emission line at $\sim$7 000 Å is MgII.

There are two more UV-excess sources (UVEXJ2026+4050 and UVEXJ2049+3811) both with a Hectospec spectrum, showing a continuum with several emission lines at the position of the Balmer lines. These emission features are probably not real since they are also present in the offset sky spectrum. Their photometry $(r-H\alpha)\sim$0.4 confirms the emission features in the spectra. The narrow Balmer and HeI emission lines, indicating a low-density environment, are mostly (or completely) from the huge diffuse emission in the field, likely a HII region.

Without the emission lines they might just be hot white dwarfs. Based on the available spectra the sources can not be classified, so they are labeled 'unknown'.

For two other UV-excess sources (UVEXJ0110+6004 and UVEXJ2047+4155) there are Calar Alto 2.2m spectra available. These UV-excess sources are not included in this paper since they are the known Cataclysmic Variables 'HT Cassiopeiae' (Rafanelli, 1979) and 'V516 Cygni' (Spogli et al., 1998).

4 DISCUSSION AND CONCLUSIONS

The main conclusion is that of the sources in the UV-excess catalogue 95% are genuine UV-excess sources, such as white dwarfs, white dwarf binaries, subdwarf stars type O and B and QSOs. Five percent of the UV-excess candidates are classified as main-sequence (MS) stars or blue horizontal branch (BHB) stars with spectral types later than A0V. If the sources classified as MS/BHB are main-sequence stars, the fitting of the Pickles library spectra (Pickles, 1998) shows that 4 sources are slightly reddened F0V stars with reddening $E(B-V)\leqslant0.1$ and 3 sources are B0V-B3V stars with reddening $0.4\leqslant E(B-V)\leqslant0.5$. Their spectra look like B-type main-sequence stars, but the Balmer absorption lines are stronger than the Balmer lines of the best fit template spectra. Since gravity is slightly high they could be horizontal branch stars, although usually BHB stars have less helium absorption. Two of the B-type MS/BHB stars slightly blue shifted so might be high velocity stars, UVEXJ1940+3220 has a velocity of RV=320km/s and UVEXJ1938+3054 has a velocity of RV=163km/s. There is 1 G-type star with as best fit a Pickles G2V star with reddening $E(B-V)\sim0.3$. G-type stars are expected to have colours redder than $(g-r)>0.6$ and $(U-g)>0.4$, but they can enter the UV-excess region when they are metal weak, i.e. subdwarfs type with less light blocked at the blue/UV wavelengths (Eracleous et al., 2002). Since the number of late type stars in the fields is large, photometric errors can cause a few outliers to be scattered into the UV-excess selection region (Krzesinski et al., 2004).

Secondly, in the colour-colour and colour-magnitude diagrams of Figs. 6 and 7 of V12 about 20% of the UV-excess sources overlaps with the location of the 'subdwarfs' population at $(g-r)>0.3$ and $(U-g)>0.2$. These UV-excess sources that overlap the subdwarf area in the colour-colour and colour-magnitude diagrams are 2 QSOs, 7 Cataclysmic Variables, 1 DAe, 2 T Tauri stars, 1 Be star, 3 DA+dM stars, 3 He-sdO stars, 1 sdO star, 2 sdB stars, 1 B-type MS/BHB star, 3 F-type MS/BHB stars and 1 DAB white dwarf. For our selection of UV-excess candidates from the *UVEX* data this means that when the aim is to find white dwarfs, a colour cut can be applied to decrease the number of other objects. But leaving these sources at the location of the 'subdwarfs' out from the UV-excess catalogue would lead to a loss of most QSOs, Cataclysmic Variables, T Tauri stars, Be stars and DA+dM stars.

The location of the different populations in the $(U-g)$ vs. $(g-r)$ colour-colour diagram and the g vs. $(U-g)$ and g vs. $(g-r)$ colour-magnitude diagrams is shown in Fig. 1 and 2. Their positions match with the positions of the populations in the colour-colour diagrams of other surveys (e.g. Fig. 1 of Krzesinski et al., 2004, Fig. 1 of Harris et al., 2003, Fig. 3 of Stobie et al., 1997, Fig. 3 of Yanny et al., 2009 and the Figs. of Kilkenny et al., 1997). The locations of the classified sources in the colour-colour and colour-magnitude diagrams agree with the locations of the sources with a Simbad match in the colour-colour and colour-magnitude diagrams in Fig. 9 of V12. There is a clear relation between the different kind of sources and the way they are selected in V12. The way the sources were selected from the colour-colour and colour-magnitude diagrams is captured in the 'selection label' (column 20 of the UV-excess catalogue, Appendix A of V12), and is summarized for our classified sources in Table. 4. Only 2 DA white dwarfs were selected less than 0.4 magnitude from the blue edge in the g vs. $(g-r)$ colour-magnitude diagram, the other 60 DA white dwarfs were selected more than 0.4 magnitude from the blue edge in the g vs. $(g-r)$ colour-magnitude diagram. All DB and DC white dwarfs were selected both were selected more than 0.4 magnitude from the blue edge in both colour-magnitude diagrams and in the $(U-g)$ vs. $(g-r)$ colour-colour diagram, while most DBA white dwarfs were selected less than 0.4 magnitude from the blue edge in the g vs. $(g-r)$ colour-magnitude diagram and in the $(U-g)$ vs. $(g-r)$ colour-colour diagram. The 2 QSOs and the majority of the Hα emission line objects were selected in the g vs. $(U-g)$ colour-magnitude diagram but not in the g vs. $(g-r)$ colour-magnitude diagram. We could improve the selection method of V12 using these spectroscopic results by taking only sources in the UV-excess catalogue with favourable selection labels into account. This will increase the number of genuine UV-excess objects to 97% by e.g. leaving out selection labels '514' and '518' since the largest fraction MS/BHB stars have these selection labels, but this will also lead to a loss of some peculiar objects such as DAe stars, Cataclysmic Variables and Be stars. The *UVEX* and *IPHAS* photometry can also be combined with other (infrared and ultraviolet) surveys in order to improve the selection of different populations (Verbeek et al., in prep.).

About 64% of the UV-excess candidates turn out to be white dwarfs. The fitting of the white dwarf models to the UV-excess hydrogen atmosphere white dwarf spectra shows a distribution of $9\,000\mathrm{K}<T_{\mathrm{eff}}<65\,000\mathrm{K}$ and an average surface gravity of $log\,g\sim8$. These results are in agreement with the results of other studies. (Liebert et al., 2005, Bergeron et al., 1992, Napiwotzki et al., 1999, Finley et al., 1997, Gianninas et al., 2011 and Kepler et al., 2007). The accuracy of the continuum fitting method applied in Sect. 3.1 depends on the SNR and the flux calibration of the spectra. For white dwarfs the accuracy of the temperature fit will approach the surface temperature to typically $\sim1\,000K$ for white dwarfs with T<20 000 and $\sim2\,000K$ for the hotter white dwarfs with T$\geqslant$20 000, for spectra with signal to noise SNR>20.

When we extrapolate the result that 64% of the

Table 4. The selection in V12 of the classified UV-excess spectra.

Label	Selected from	Objects
514	g vs. $(U-g)$	1DAe, 1Be, 1MS/BHB, 1He-sdO, 1sdB+F
515	g vs. $(U-g)$ & $(U-g)$ vs. $(g-r)$	2CV, 2QSO, 1TT, 1DAB+dM, 1He-sdO, 1BHB/MS
518	g vs. $(U-g)$ & $<0.4g$ vs. $(g-r)$	1CV, 1DAe, 2MS/BHB, 1noisy
519	g vs. $(U-g)$ & $<0.4g$ vs. $(g-r)$ & $(U-g)$ vs. $(g-r)$	5CV, 4DBA, 2DA, 1TT, 2DA+dM, 4sdB, 2He-sdO, 1BHB/MS, 1G, 4noisy
1028	g vs. $(g-r)$	28DA, 1DZA, 1unknown, 1DA+dM, 1MS/BHB, 1sdB, 1noisy
1029	g vs. $(g-r)$ & $(U-g)$ vs. $(g-r)$	3DA, 1DA+dM
1031	g vs. $(g-r)$ & $<0.4g$ vs. $(U-g)$ & $(U-g)$ vs. $(g-r)$	1DA, 1MIII
1542	g vs. $(g-r)$ & g vs. $(U-g)$	1unknown
1543	g vs. $(g-r)$ & g vs. $(U-g)$ & $(U-g)$ vs. $(g-r)$	28DA, 4DB, 1DBA, 4DC, 1DAe, 1DZ, 1sdO, 1BHB/MS, 6noisy

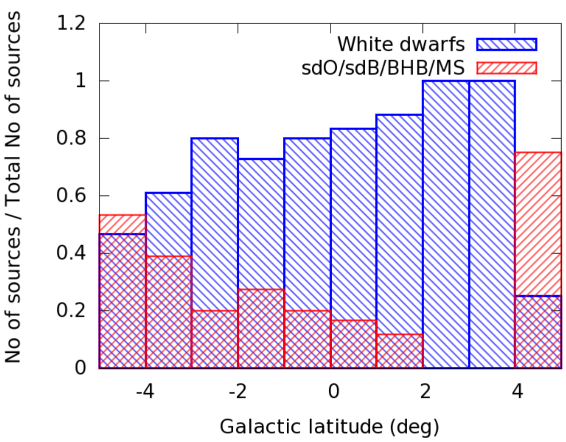

Figure 9. Galactic latitude distribution of the sources classified as white dwarfs (blue) and the sources classified as sdO/sdB stars, MS/BHB stars and "noisy" (red). The number of sources per bin is normalized by the total number of obtained spectra in the latitude bin.

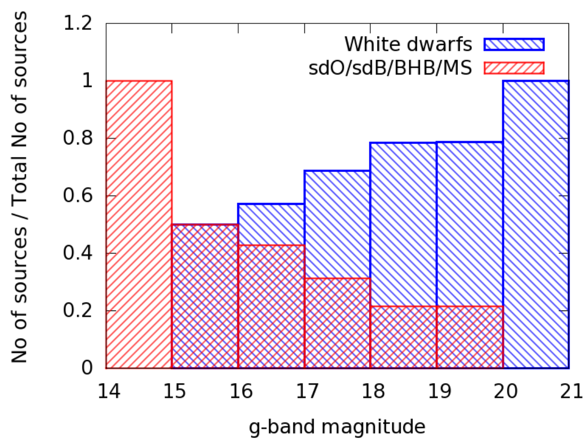

Figure 10. Magnitude distribution of the sources classified as white dwarfs (blue) and the sources classified as sdO/sdB stars, MS/BHB stars and "noisy" (red). The number of sources per bin is normalized by the total number of obtained spectra in the magnitude bin.

UV-excess catalogue sources are white dwarfs, the complete *UVEX* survey will bring up a sample of $\sim 1.2 \times 10^4$ new white dwarfs (~7 per square degree). If we only look at UV-excess white dwarf sample brighter than g<20, *UVEX* will bring up a sample of ~4000 new white dwarfs with g<20 in the full survey area. The UV-excess sample might not be complete for the coolest white dwarfs below T<10 000K since they have too red colours. There is also the additional problem of dust extinction (Sale et al., 2009), which has only a small effect on the local white dwarf sample while it merely screens out more distant objects. As shown in Sect. 3.1 reddening is typically $E(B-V)\leqslant 0.1$ magnitudes for most of the white dwarfs in the UV-excess catalogue. A space density of white dwarfs (Holberg et al., 2008) in the Galactic Plane and a comparison with population synthesis predictions will be further discussed in Verbeek et al., (in prep.).

The Galactic latitude distribution of the sources classified as white dwarfs and as sdO/sdB stars, main-sequence stars and blue horizontal branch stars is shown in Fig. 9. The sources labeled as "noisy" in Sect. 3.2 are add to the sdO/sdB/BHB/MS sample since they probably are sdO/sdB or MS/BHB stars. The white dwarfs are mainly detected at Galactic latitudes smaller than $|b|$<4, while the distribution of sdO/sdB stars and MS/BHB stars peaks at Galactic latitudes larger than $|b|$>4. This result can be explained by the absolute magnitude distribution of the different populations in combination with the effect of extinction, as can be seen in Fig. 1 of Groot et al. (2009).

The magnitude distribution of the spectra classified as white dwarfs and as sdO/sdB stars, MS/BHB stars and "noisy" is shown in Fig. 10. The fraction of white dwarfs clearly increases for fainter g-band magnitudes. The total number of white dwarfs increases strongly for fainter magnitudes since also the number of selected sources increases (see e.g. Fig. 7 of V12 and Fig. 1 of Bergeron et al., 1992). The fraction of MS/BHB and subdwarf sources is larger for the brighter g-band magnitudes, even with the sources classified as "noisy" included in the sdO/sdB/BHB/MS sample. A larger fraction of white dwarfs is found at magnitudes fainter than g>17.

If we assume that UV-excess candidates classified as main-sequence stars and blue horizontal branch stars are all MS stars, we can estimate the distance d using $d{=}10^{0.2\times(m-M-A_V)}\,10pc$, where we use the observed g-band magnitude as apparent magnitude (m), M is the absolute magnitude and $A(V)$ is the total extinction for the V-band filter. Since $A(V) = R_V \times E(B-V)$, where we use R_V=3.1 for the indicator of dust grain size distribution

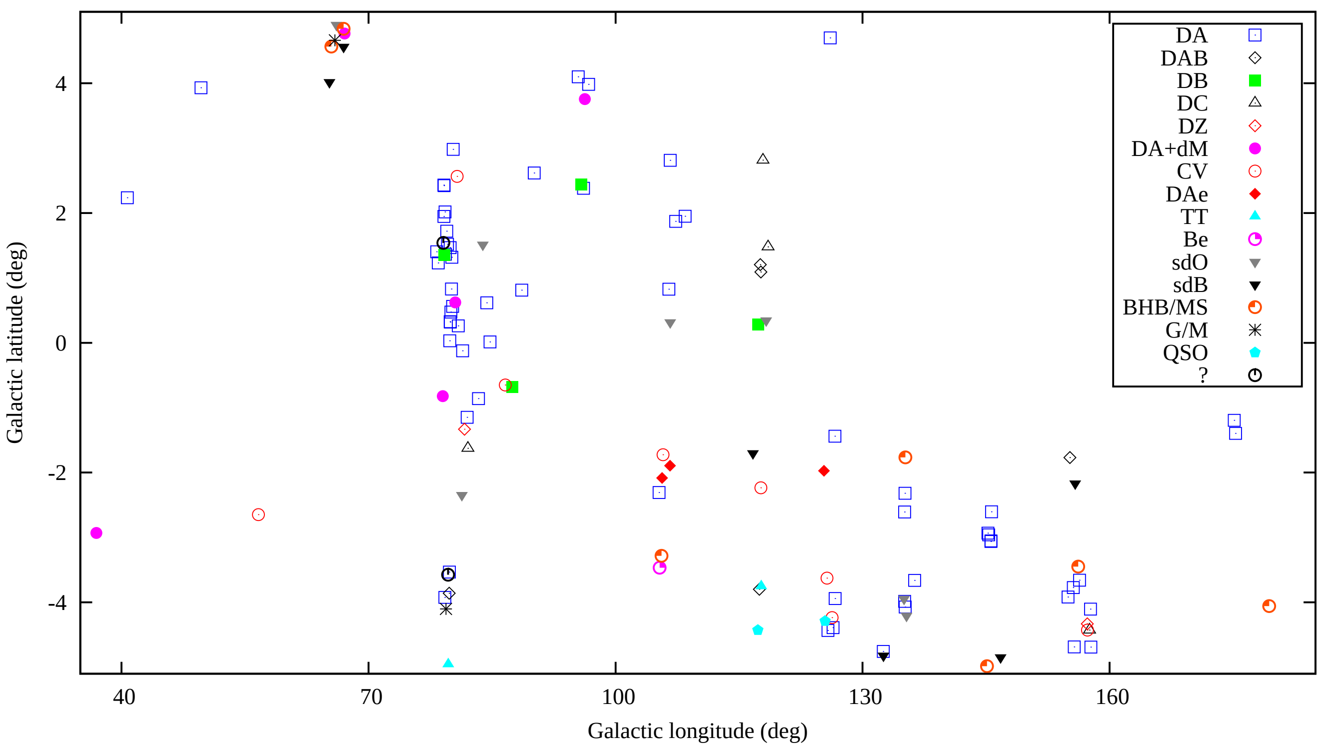

Figure 11. Galactic latitude vs. Galactic longitude diagram with all obtained UV-excess spectra. The classified sources are indicated with the symbols of Figs. 1 to 3.

and the results of the fitting in Sect. 3.2 for the reddening $E(B-V)=A(B)-A(V)$, we can estimate a distance range per source. In our UV-excess sample the F-type MS/BHB stars have a g-band magnitude of $17.3<g<19.6$ and reddening $E(B-V)=0.1$, the G2V star has a g-band magnitude of $g=19.5$ and $E(B-V)=0.3$, the B-type BHB/MS stars have a typical g-band magnitude between $14.5<g<18.6$ and $E(B-V)=0.4$, Taking into account the effect of reddening the distance estimations would be ∼5kpc for the G2V star with $g=19.5$ and ∼8kpc for the F0V star with $g=17.3$ which is within the Milky Way. For the fainter F-type and B-type stars the distances would be ∼20kpc for the F0V star with $g=19.6$ and ∼35kpc for the B0V star with $g=17.0$ if they would be main-sequence stars. These distances would be outside the Milky Way. Since their colours are only slightly reddened they must be intrinsically fainter objects. So, we conclude that these objects must be blue horizontal branch stars or subdwarf type stars.

An interesting side benefit is the detection of the 2 broadline QSOs in the UV-excess spectra, with $z\sim2.16$ and $z\sim1.48$ and at $|b|=4$. Only about ∼10 QSOs are found at low Galactic latitude regions (Im et al., 2007, Lee et al., 2008 and Becker et al., 1990). The Schlegel map (Schlegel et al., 1998) gives a reddening of $E(B-V)\sim0.5$ for both QSOs. Due to the internal reddening of the QSOs we can not directly estimate the amount of reddening caused by our Milky Way from their spectra (Knigge et al., 2008).

Of the UV-excess spectra 122 have a match in *IPHAS* . These matches are shown in the colour-colour and colour-magnitude diagrams of Fig. 3. Nine of the classified UV-excess sources are in the Deacon IPHAS-POSSI PM catalogue (Deacon et al., 2009): 7 DA white dwarfs, 1 DC white dwarf and 1 DA+dM binary system. Except for the DA+dM at $(r-i)=1.3$ all sources overlap with the location of the white dwarf population at $(r-i)\sim0$ in Fig. 11 of V12. Eight of the classified UV-excess sources are in the Witham Hα emission line catalogue (Witham et al., 2008): 4 Cataclysmic Variables, 1 Be star, 1 Classical T Tauri star and 2 sdO candidates. There are some sources with clear Hα emission lines in their spectra that are not in the Witham Hα emission line catalogue. Four sources classified as Cataclysmic Variables clearly show Hα emission in the *IPHAS* colour-colour diagram of Fig. 3. Two of these Cataclysmic Variables are not in the Witham catalogue because they have r-band magnitudes $r>19.5$. The Hα emission of some other Cataclysmic Variables with $EW<20$Å is probably not strong enough to be in the Witham catalogue, or they can also have variable emission.

4.1 Comparison with spectroscopic surveys

• We can compare our results with the spectroscopic observations of Eracleous et al. (2002) of 27 UV-bright stars, with $(U-B)<-0.2$ and magnitude $13<B<16$, selected from the Sandage Two-colour Galactic Plane survey, in the Lanning catalogue (Lanning, 1973). This sample contains 2 DA white dwarfs, 1 DB white dwarfs, 1 DA+dM, 16 O/B stars (60%), 1 F/G star, 1 M star, 1 sdO, 2 subdwarfs, 1 composite object and 1 emission line star. When we compare this sample with the sources in our UV-excess sample the distribution of spectral types is similar. The fraction of white dwarfs and O/B stars is very different for both surveys, which might be due to the magnitude limit 13<B<16 of the Sandage survey and the criteria used for the classification.

- A second sample of 46 UV-bright sources from the Sandage Two-color Survey obtained by Lépine et al. (2011) contains 29 DA white dwarfs (63%), 5 DB white dwarfs (11%), 3 DC white dwarfs, 1 DZ white dwarf, 1 DA+dM, 1 sdB, 2 sdO and 4 F-type stars. Here the F-type stars are at Galactic latitudes larger than $|b| > 5$. When we compare this sample with the sources in the UV-excess sample the distribution of spectral types and their variety is very similar, e.g. fraction of white dwarfs. The number of Hα emission line objects in the Sandage survey is very different from our UV-excess sample.

- The Kitt Peak-Downes (KPD) survey (Downes et al., 1986) sample of 158 UV-excess objects at Galactic latitude $|b|<12^{\circ}$, brighter than B<15.3 and $(U-B)$<–0.5 contains 21 DA white dwarfs, 13 white dwarfs of other types, 20 sdO, 40 sdB, 5 Planetary Nebulae, 41 Be stars, 9 Cataclysmic Variables and 9 other peculiar sources. Remarkable is the small fraction of white dwarfs (only 22%) and the high number of Be stars and Planetary Nebulae in the KPD survey compared to the *UVEX* survey. This might be partly due to the Galactic latitude difference of the two surveys and the fact that the detection of Planetary Nebulae is strongly affected by interstellar obscuration (Fig. 6 of Miszalski et al., 2008, Fig. 7 of Parker et al., 2006 and Moe and De Marco, 2006) at Galactic latitudes smaller than $|b|<5$. Normally narrow-band and red/IR surveys would be required to select new Planetary Nebulae. The low number of main-sequence sources in the KPD survey can be explained by the demand $(U-B)$<–0.5 and their classification of all blue continuum spectra with strong Balmer lines as sdB candidates. This also directly explains why the number of sdO and sdB stars in KPD is reversed compared to *UVEX* . Despite the different magnitude depths and colour cuts the fraction of e.g. QSOs, Cataclysmic Variables and DC white dwarfs is the same for both surveys. The distribution of different spectral types over Galactic latitude and Galactic longitude varies strongly as can be seen in Fig. 11. When we compare only the KPD sources at Galactic latitude smaller than $|b| <5$ and do not take the Hα emitters into account, the result is 16 DA, 2 DB, 1 DC, 13 sdB and 4 sdO stars. This result is similar to our classified UV-excess spectra.

ACKNOWLEDGEMENT

This paper makes use of data collected at the Isaac Newton Telescope, operated on the island of La Palma by the Isaac Newton Group in the Spanish Observatorio del Roque de los Muchachos of the Instítuto de Astrofísica de Canarias. The observations were processed by the Cambridge Astronomy Survey Unit (CASU) at the Institute of Astronomy, University of Cambridge. Hectospec observations shown in this paper were obtained at the MMT Observatory, a joint facility of the University of Arizona and the Smithsonian Institution. The *IPHAS* FAST spectra shown in this work were obtained at Fred Lawrence Whipple Observatory (FLWO) on Mount Hopkins, Arizona. We gratefully acknowledge the *IPHAS* consortium for making available the Hectospec and FAST observations. This research has made use of the Simbad database and the VizieR catalogue access tool, operated at CDS, Strasbourg, France. KV is supported by a NWO-EW grant 614.000.601 to PJG. The authors would like to thank Detlev Koester and Pierre Bergeron for making available their white dwarf model spectra.

REFERENCES

Aungwerojwit A., Gänsicke B.T., Rodriguez-Gil P., et al., 2005, A&A 443, 995A

Barentsen G., Vink J.S., Drew J.E., Greimel R. et al., 2011, MNRAS 415, 103B

Bergeron P., Saffer R.A., Liebert J., 1992, ApJ 394, 228B

Bergeron P., Wesemael F. & Beauchamp A., 1995, PASP 107, 1047

Brunzendorf J. & Meusinger H., 2002, A&A 390, 879B

Cardelli J.A., Clayton G.C. & Mathis J.S., 1989, ApJ 345, 245

Christlieb N., Wisotzki L., Reimers D., et al., 2001, A&A 366, 898C

Corradi R. L. M., Valentini M., Munari U., Drew J. E., et al., 2010, A&A 509, 41

Cutri R. M., Skrutskie M. F., van Dyk S. et al., 2003, yCat 2246, 0

Deacon N. R., Groot P. J., Drew J. E., et al., 2009, MNRAS 397, 1685

Demers S., Beland S., Kibblewhite E.J., et al., 1986, AJ 92, 878D

Drew J., Greimel R., Irwin M., et al., 2005, MNRAS 362, 753 (D05)

Downes R. A., 1986, ApJS 61, 569D

Eisenstein D. J., Liebert J., Harris H. C., et al., 2006, ApJ 167, 40E

Eracleous M., Wade R. A., Mateen M., et al., 2002, PASP 114, 207E

Fabricant D., Cheimets P., Caldwell N., et al., 1998, PASP 110,79F

Fabricant et al., 2004, SPIE 5492, 767F

Fabricant D., Fata R., Rollet J., et al., 2005

Finley D.S., Koester D. & Basri G., 1997, ApJ 488, 375F

Gänsicke B.T., Dillon M., Southworth J., et al., 2009, MNRAS 397, 2170G

Gianninas A., Bergeron P., Ruiz M. T., 2011, ApJ 743, 138G

Girven J., Gänsicke B.T., Steeghs D. & Koester D., 2011, MNRAS 417, 1210G

González-Solares E.A., Walton N.A., Greimel R., Drew, J.E., et al., 2008, MNRAS 388, 89

Green R. F., Schmidt M., Liebert J., 1986, ApJS 61, 305G

Greiss S., Steeghs D., Gänsicke B.T., Martn E.L., Groot P.J. et al., 2012, arXiv1202.6333G

Groot P.J., Verbeek K., Greimel R., et al., 2009, MNRAS 399, 323G

Hagen H.-J., Groote D., Engels D., Reimers, D., 1995, A&AS 111,195H

Harris H.C., Liebert J., Kleinman S.J. et al., 2003, AJ 126, 1023H

Holberg J.B., Sion E.M., Oswalt T., McCook G.P. et al., 2008, AJ 135,1225H

Homeier D., Koester D., Hagen H.J., et al., 1998 A&A 338, 563H

Im Myungshin, Lee Induk., Yunseok C., et al. 2007, ApJ 664,64

Kepler S.O., Kleinman S.J., Nitta A., Koester D. et al., 2007, MNRAS 375, 1315K

Kilkenny D., O'Donoghue D, Koen C., et al., 1997, MNRAS 287, 867K

Knigge C, Scaringi S, Goad M.R., Cottis C.E., 2008, MNRAS 386, 1426K

Koester D., et al., 2001, A&A, 378, 556

Krzesinski J., Nitta A., Kleinman S.J. et al., 2004, A&A 417, 1093K

Lamontagne R., Demers S., Wesemael F., et al., 2000, AJ 119, 241L

Lanning H.H., 1973, PASP 85, 70L

Lanning H. H., 1982, ApJ 253,752L

Lanning H. H., Meakes, M., 2004, PASP 116,1039L

Lee Induk, Im Myungshin, Kim Minjin et al., 2008, ApJS 175, 116L

Lépine S., Bergeron P., Lanning H. H., 2011, AJ 141, 96L

Liebert J., Bergeron P., Holberg J. B., 2005, ApJS 156, 47L

Limoges M., Bergeron P., 2010, ApJ 714, 1037L

McCook G. P., Sion E. M., 1999, ApJS 121, 1M

Miszalski B., Parker Q.A., Acker A. et al., 2008, MNRAS 384, 525M

Moe M., De Marco O., 2006, ApJ 650, 916

Moehler S., Richtler T., de Boer K.S. et al., 1990, A&AS 86, 53M

Morales-Rueda L. & Marsh T.R., 2002, MNRAS 332, 814M

Morgan W.W., Keenan P.C., Kellman E., 1943, QB881, M6

Napiwotzki R., 1997, A&A 322, 256N

Napiwotzki R., Green P.J., Saffer R.A., 1999, ApJ 517, 399N

Napiwotzki R., Christlieb N., Drechsel H., et al., 2003, Msngr 112, 25N

Nelemans G., Portegies Zwart S. F., Verbunt F., Yungelson L. R., 2001, A&A 368, 939N

Østensen R.H., Silvotti R., Charpinet S., et al., 2011, MNRAS 414, 2860O

Parker Q.A., Acker A., Frew D.J. et al., 2006, MNRAS 373, 79P

Pickles A.J., 1998, PASP 110, 863

Rafanelli P., 1979, A&A 76, 365R

Roeser S., Demleitner M. and Schilbach E., 2010, AJ 139,2440R

Sale S., Drew J., Unruh Y., et al., 2009, MNRAS 392, 497

Schlegel D.J., Finkbeiner D.P. & Davis, M., 1998, ApJ 500, 525

Silvestri N M., Hawley S.L., West A.A., Szkody P. et al., 2006, AJ 131, 1674S

Sion E.M., Greenstein J.L., Landstreet J.D., Liebert J., et al., 1983, ApJ 269, 253S

Sion E.M., Kenyon S.J., Aannestad P.A., 1990, ApJS 72,707S

Spogli C., Fiorucci M. & Tosti G., 1998, A&AS 130, 485S

Stobie R.S., Morgan D.H., Bhatia R.K., et al., 1987, fbs conf, 493S

Stobie R.S., Kilkenny D., O'Donoghue D., et al., 1997, MNRAS 287, 848S

Szkody P., Henden A., Mannikko L., 2007, AJ 134, 185S

Tappert C., Gänsicke B.T., Zorotovic M., et al., 2009, A&A 504, 491T

Verbeek K., Groot P.J., de Groot E., Scaringi S., Drew J.E., et al., 2012, MNRAS 420, 1115V

Vink J.S., Drew J.E., Steeghs D., Wright N.J., 2008, MNRAS 387, 308V

Wegner G., McMahan R.K., Boley F.I., 1987, AJ 94, 1271W

Wesemael F., Greenstein J.L., Liebert J., et al., 1993, PASP 105, 761W
Wisotzki L., Koehler T., Groote D. & Reimers D., 1996, A&AS 115, 227W
Witham A.R., Knigge C., Drew J.E., et al., 2008, MNRAS 384, 1277
Yanny B., Rockosi C., Newberg H.J., et al., 2009, AJ 137, 4377
York D.G., Adelman J., Anderson J.E. et al., 2000, AJ 120, 1579Y

APPENDIX A: LIST OF OBTAINED UV-EXCESS SPECTRA

All UV-excess spectra, their features and classification are summarized in Table AA1, sorted by right ascension. The columns contain the spectrum number and name composed of the *UVEX* right ascension and declination, the Galactic longitude and latitude, the *UVEX* field in which the object was selected, the *UVEX* selection label (column 20 of the UV-excess catalogue, described in V12), the *UVEX* photometry, if available the *IPHAS* photometry, the observing run and the classification. The classification is summarized in the two last columns. Column 14 shows the type of object and the "by eye" most appropriate spectral type of the spectrum. Sources which have no good fitting result are labeled as "noisy" in column 14. Column 15 shows the result of the spectra fitting: for white dwarfs the effective temperature $T_{\rm eff}$ in kK and if available the surface gravity $log\, g$. For He-sdO, sdO, sdB and BHB/MS B-type sources column 15 shows $T_{\rm eff}$ in kK, $log\, g$ and $log\,(n(He)/n(H))$ and for F-type MS/BHB sources without He lines $T_{\rm eff}$ in kK and $log\, g$. For sources classified as MS/BHB and for most sources labeled as "noisy" column 15 shows the most appropriate main-sequence spectral type and reddening $E(B-V)$. For the Hα emission line stars column 15 shows the $FWHM$ and EW of the $H\alpha$ line given in units of Å.

All obtained UV-excess spectra are shown in Figs. A1 to A11 per population sorted by right ascension. These spectra and Table AA1 can also be obtained from the *UVEX* website. Note that the Hectospec spectra might show emission features at the wavelengths of the Balmer lines due to bad sky subtraction in fields with diffuse emission (Fabricant et al., 2005). The Hectospec spectra were corrected for incomplete sky subtraction (Vink et al., 2008), and they are not flux calibrated. Some of the WHT/ISIS spectra obtained in December 2010 have a small hump around 5 100Å. which is not a real feature. Also note the dichroic gap from λ=5 200–5 600Å, of the WHT/ISIS spectra due to the blue and red arm of ISIS. All UV-excess spectra were smoothed by a boxcar smoothing algorithm which takes for each pixel also the flux of four neighbouring pixels into account with weights 1:2:4:2:1.

A1 Notes to individual objects

- UVEXJ001102.23+584232.3: Classified as T Tauri candidate with underlying M4V atmosphere. CaII emission and strong hydrogen lines where $H\alpha$ has $FWHM$=6Å and EW=–80Å

- UVEXJ011053.07+604830.9: Classified as DAe white dwarf, showing narrow Hα, Hβ and Hγ emission lines in broad absorption lines with additionally HeI emission, so could also be a Dwarf Nova. No sign of a companion.

- UVEXJ012359.82+672223.1: DA white dwarf. The bump at λ=6 300Å is due to the data calibration.

- UVEXJ041926.84+440058.4: DC white dwarf, showing a very blue continuum spectrum and possibly some weak HeI absorption.

- UVEXJ041045.70+461137.1: Only a blue WHT/ISIS spectrum was obtained for this source, sufficient to clearly classify the source as a DA white dwarf.

- UVEXJ041840.30+441714.1: DZ white dwarf showing a continuum with clear CaII H and K absorption in combination with weak hydrogen and HeI absorption lines, similar to the DZ spectra of Sion et al. (1990).

- UVEXJ202457.34+410804.1: There is a gap in the red spectrum at λ=7 500Å. The absorption features at λ=6 200Å are not real.

- UVEXJ202630.19+405024.1: Classified as 'unknown'. The Balmer and HeI emission lines in the spectrum of this source are also present in the sky offset spectrum due to diffuse emission in the field.

- UVEXJ202712.06+424720.1: Novalike CV with broad, double peaked Balmer and Helium lines.

- UVEXJ202744.63+405044.5: DB white dwarf. The Hα and Hβ emission lines are not real.

- UVEXJ202800.47+405620.0: Hα nebula structure around object in *IPHAS* finders.

- UVEXJ203656.54+392934.9: Classified as 'noisy', has a white dwarf type spectrum showing several odd lines. There is a nearby red star on the *IPHAS* images.

- UVEXJ204649.51+410906.2: DZ white dwarf with clear CaII H&K and no other lines. The Hα line is not real.

- UVEXJ204710.61+413133.5: Unclear features in the red part of the spectrum, which may be due to a red companion. Remarkable: this source is the bluest DA in Fig. 1 while it has $(HeI-r)$=0.23.

- UVEXJ204751.27+442920.1: Odd shaped Balmer lines and unclear features in the red part of the spectrum, which may be due to a red companion.

- UVEXJ204923.48+381139.0: Classified as 'unknown'. The emission lines are also present in the sky offset spectrum. These lines are mostly (or completely) due to huge diffuse emission in the field. The sources has a match in the IPHAS-POSS PM catalogue (Deacon et al., 2009). This indicates that the sources must be an evolved stellar objects within the Milky Way.

- UVEXJ204945.83+382057.2: DA white dwarf. Red part of the spectrum too noisy (faint source g=19.7).

- UVEXJ205039.07+373958.4: M-giant with type M5III showing clear TiO bands. No sign of a companion is found in the blue part of the spectrum. Without a white dwarf companion normally these type of objects are found at $(g-r)\sim1.5$.

- UVEXJ205449.65+371953.2: T Tauri candidate with underlying M5V atmosphere. Weak hydrogen lines where $H\alpha$ has $FWHM$=4Å and EW=–9Å, due to low mass accretion (Fig.1 of Barentsen et al., 2012).

- UVEXJ224112.21+564419.1: CV with broad Balmer and Helium lines, including He II 4686: could be magnetic.

- UVEXJ224145.94+562230.0: Classified as DAe, could be a Dwarf Nova, showing narrow Hα emission and broad Balmer absorption lines.

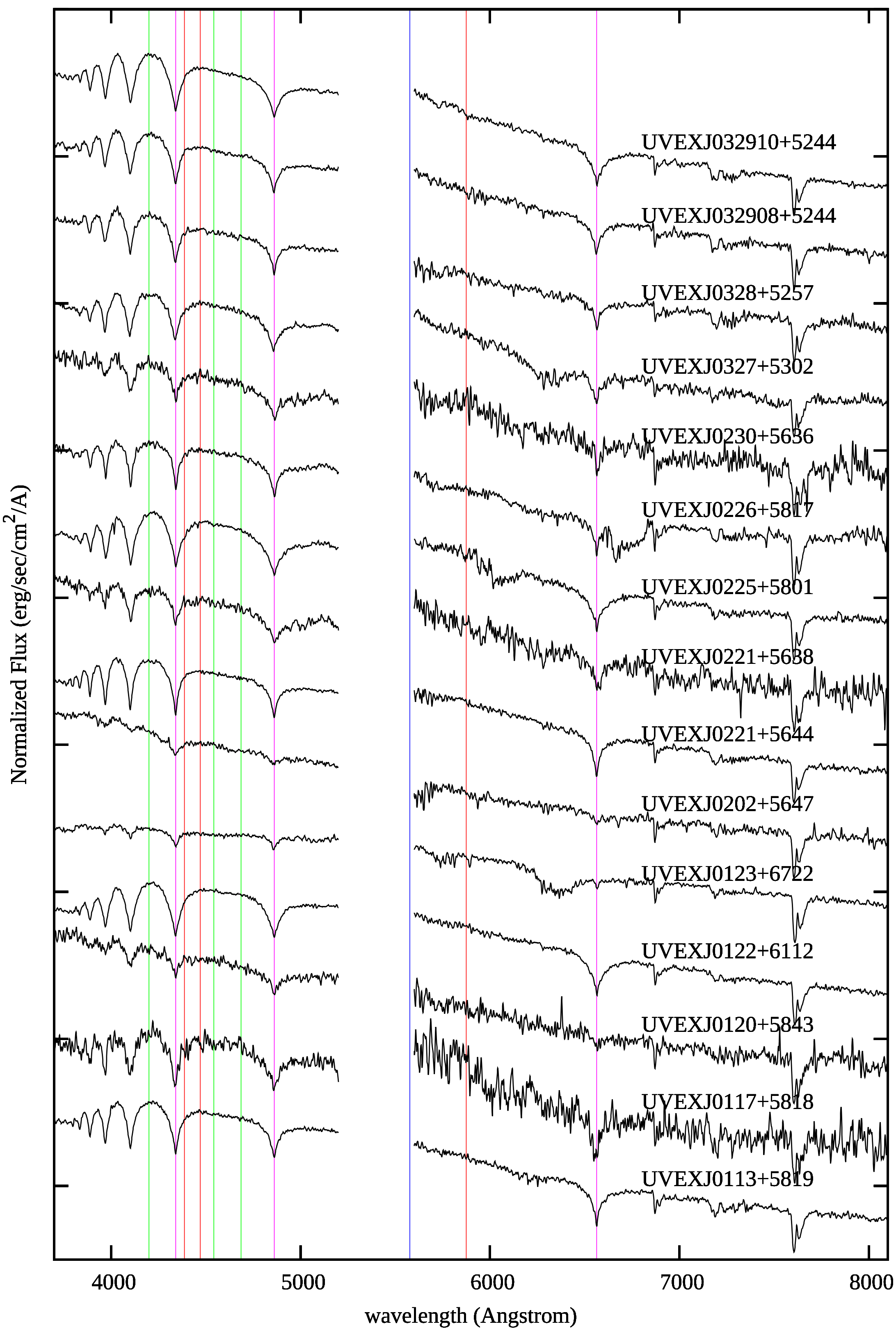

Figure A1. DA white dwarfs. The pink, red and green lines indicate the position of hydrogen, HeI and HeII respectively. The blue line is a skyline in the Hectospec spectra.

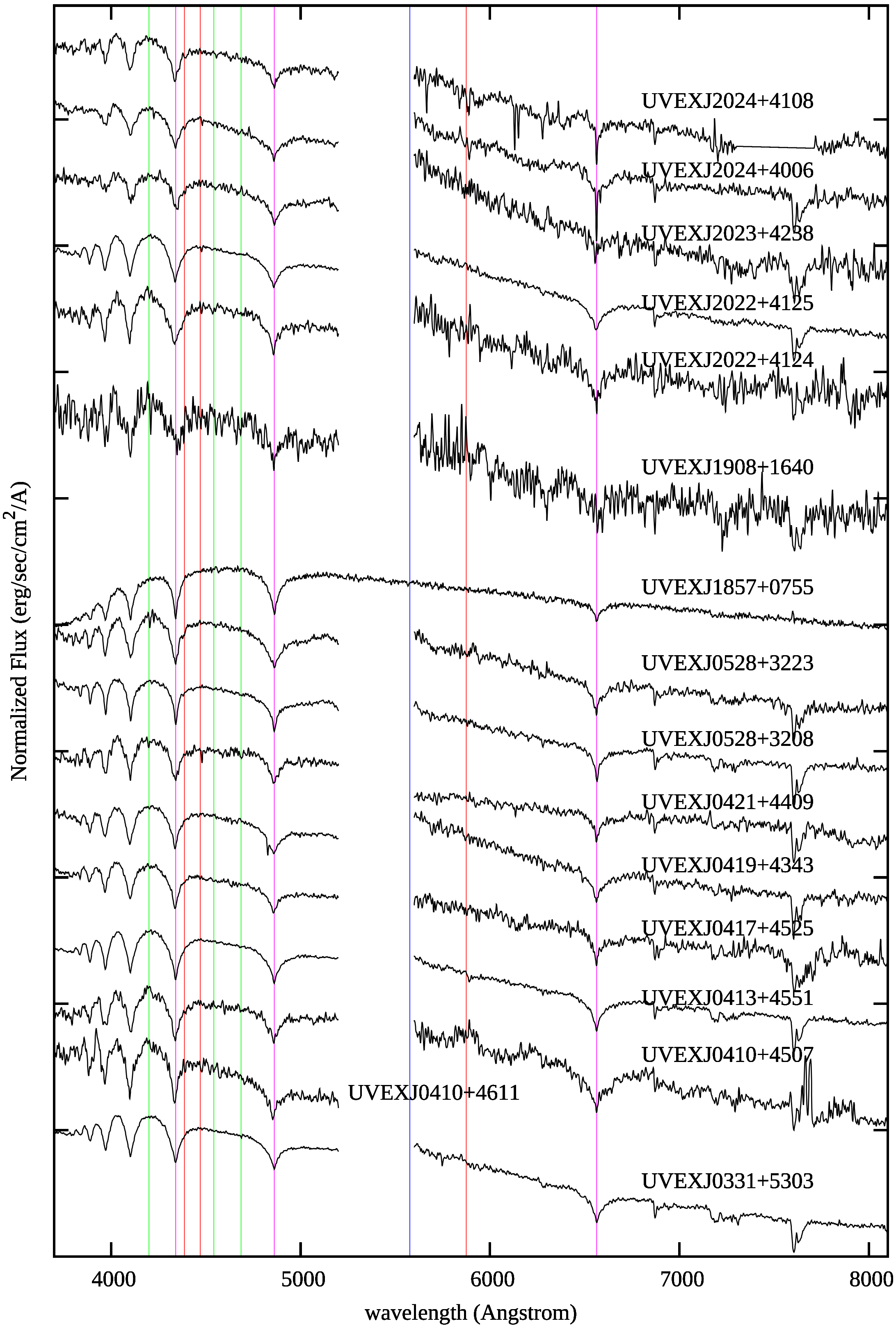

Figure A2. DA white dwarfs. The pink, red and green lines indicate the position of hydrogen, HeI and HeII respectively. The blue line is a skyline in the Hectospec spectra.

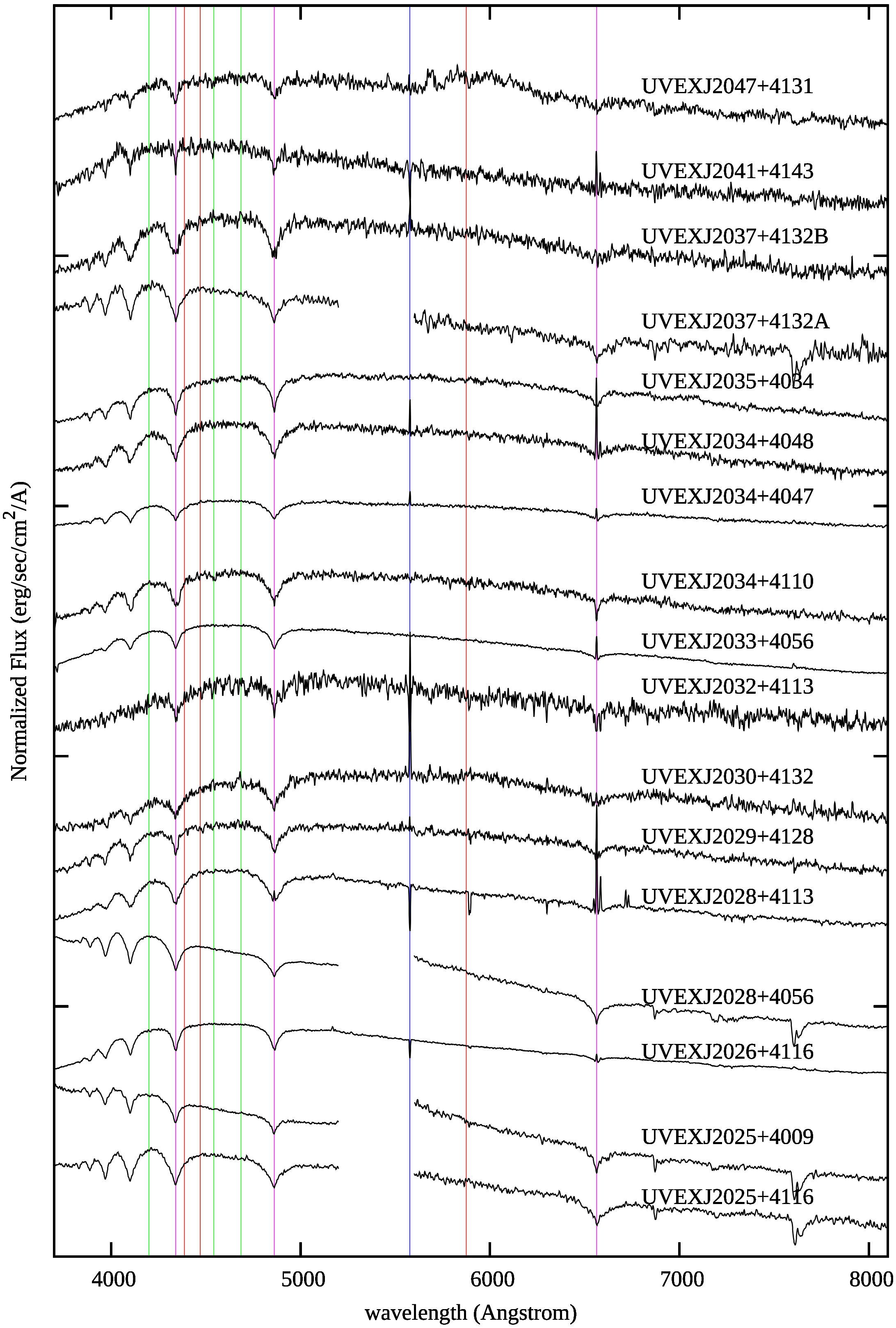

Figure A3. DA white dwarfs. The pink, red and green lines indicate the position of hydrogen, HeI and HeII respectively. The blue line is a skyline in the Hectospec spectra.

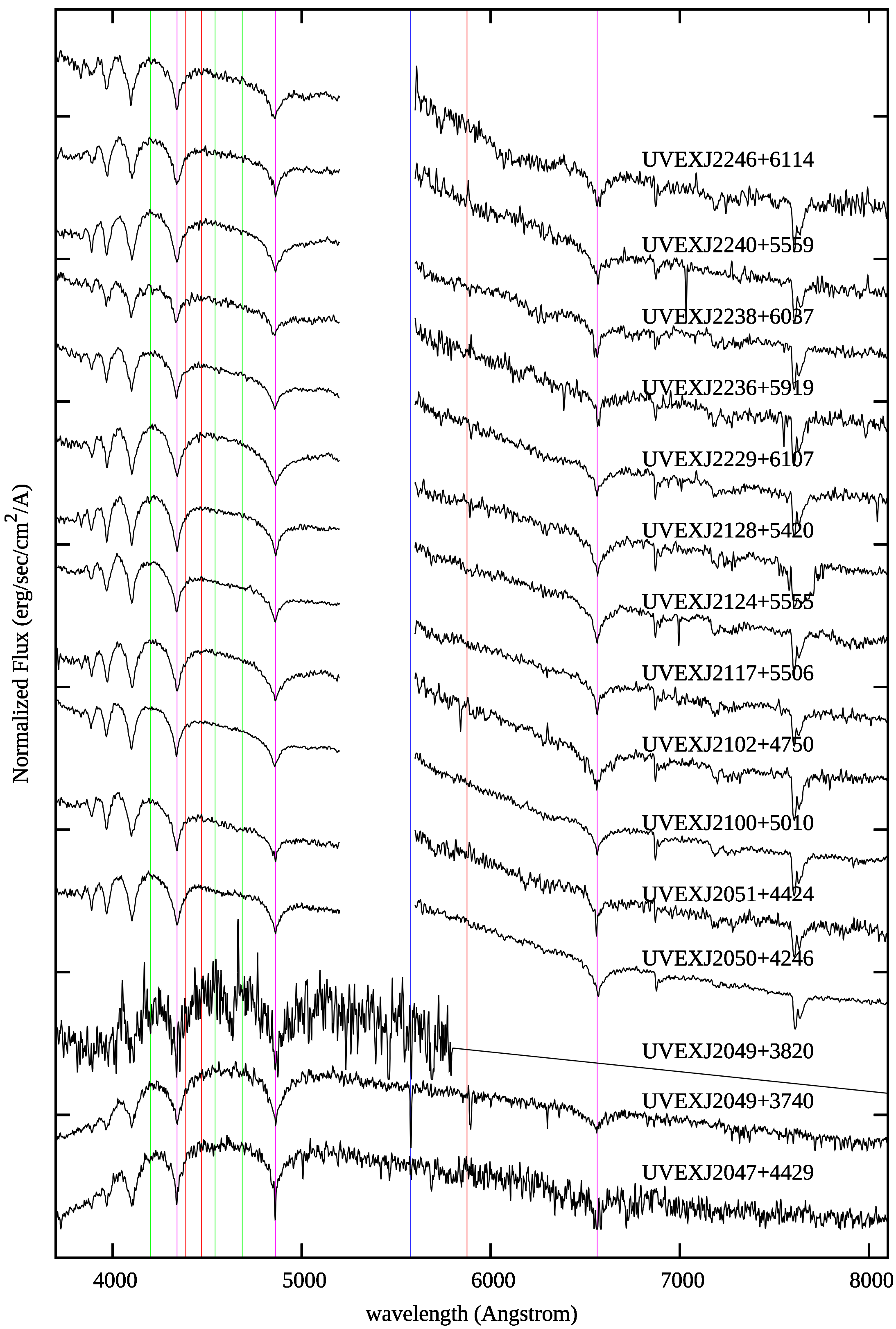

Figure A4. DA white dwarfs. The pink, red and green lines indicate the position of hydrogen, HeI and HeII respectively. The blue line is a skyline in the Hectospec spectra.

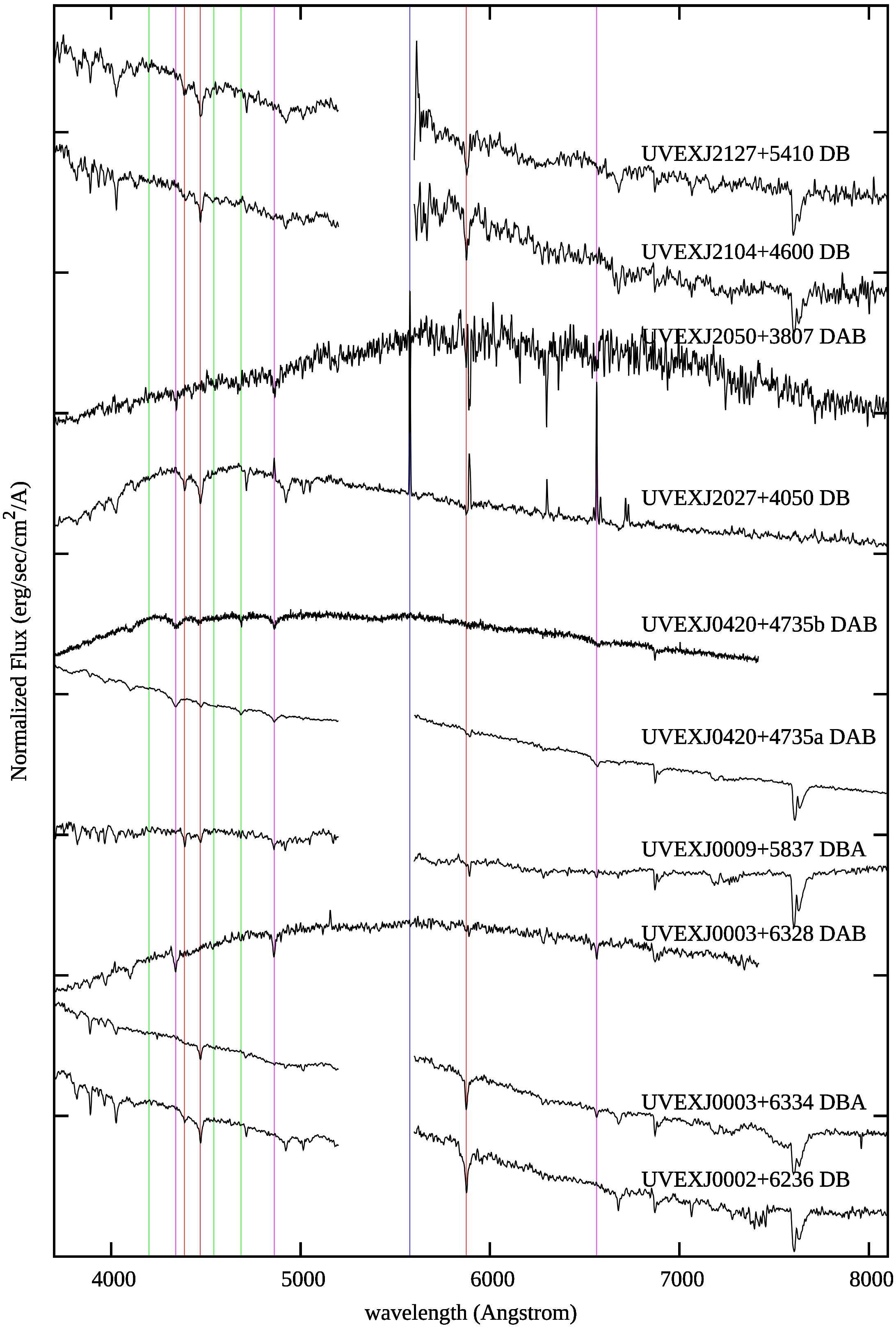

Figure A5. All UV-excess spectra classified as DB and DAB white dwarfs. The pink, red and green lines indicate the position of hydrogen, HeI and HeII respectively. The blue line is a skyline in the Hectospec spectra.

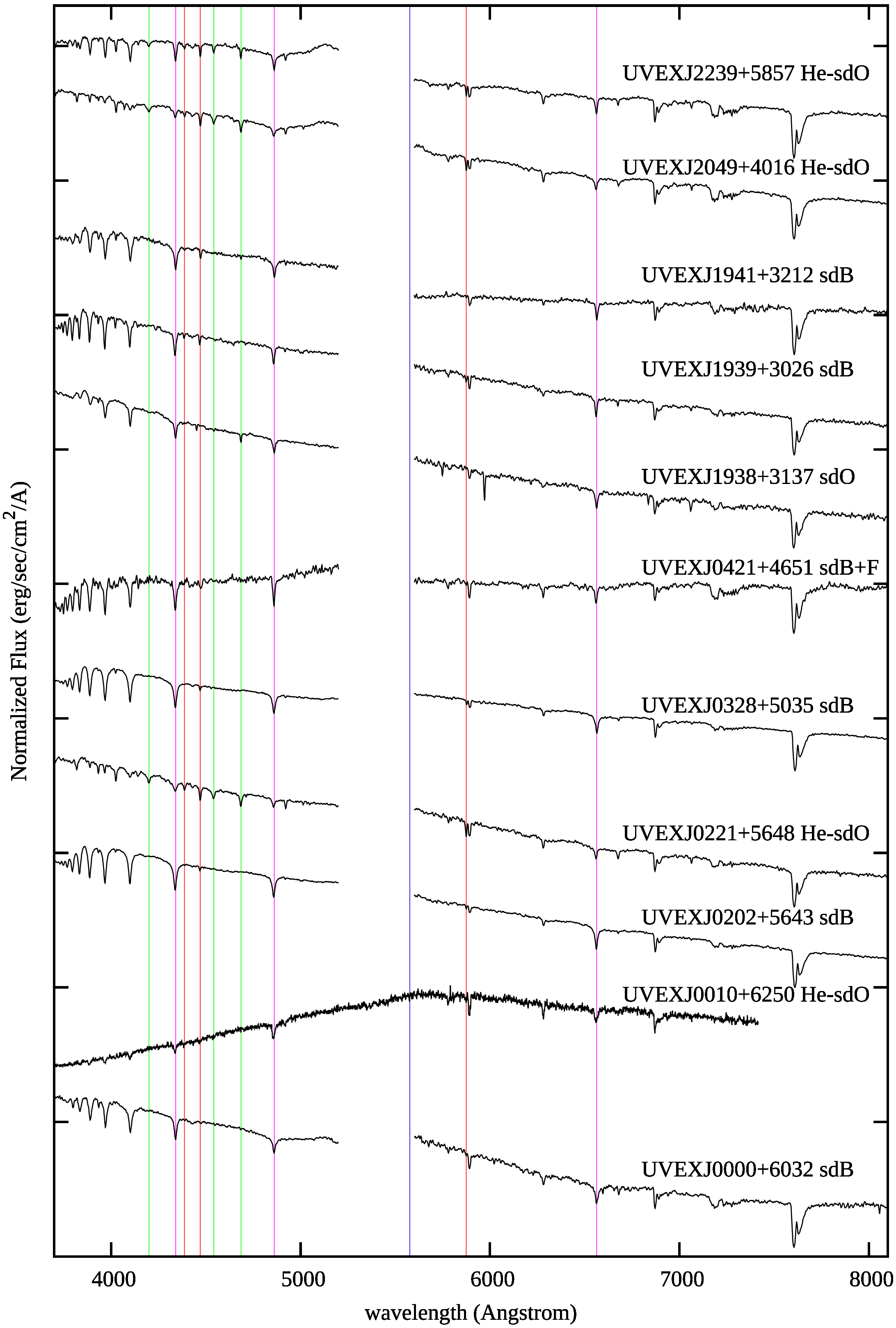

Figure A6. The UV-excess spectra classified as He-sdO, sdO, sdB and sdB+F candidates. The pink, red and green lines indicate the position of hydrogen, HeI and HeII respectively. The blue line is a skyline in the Hectospec spectra.

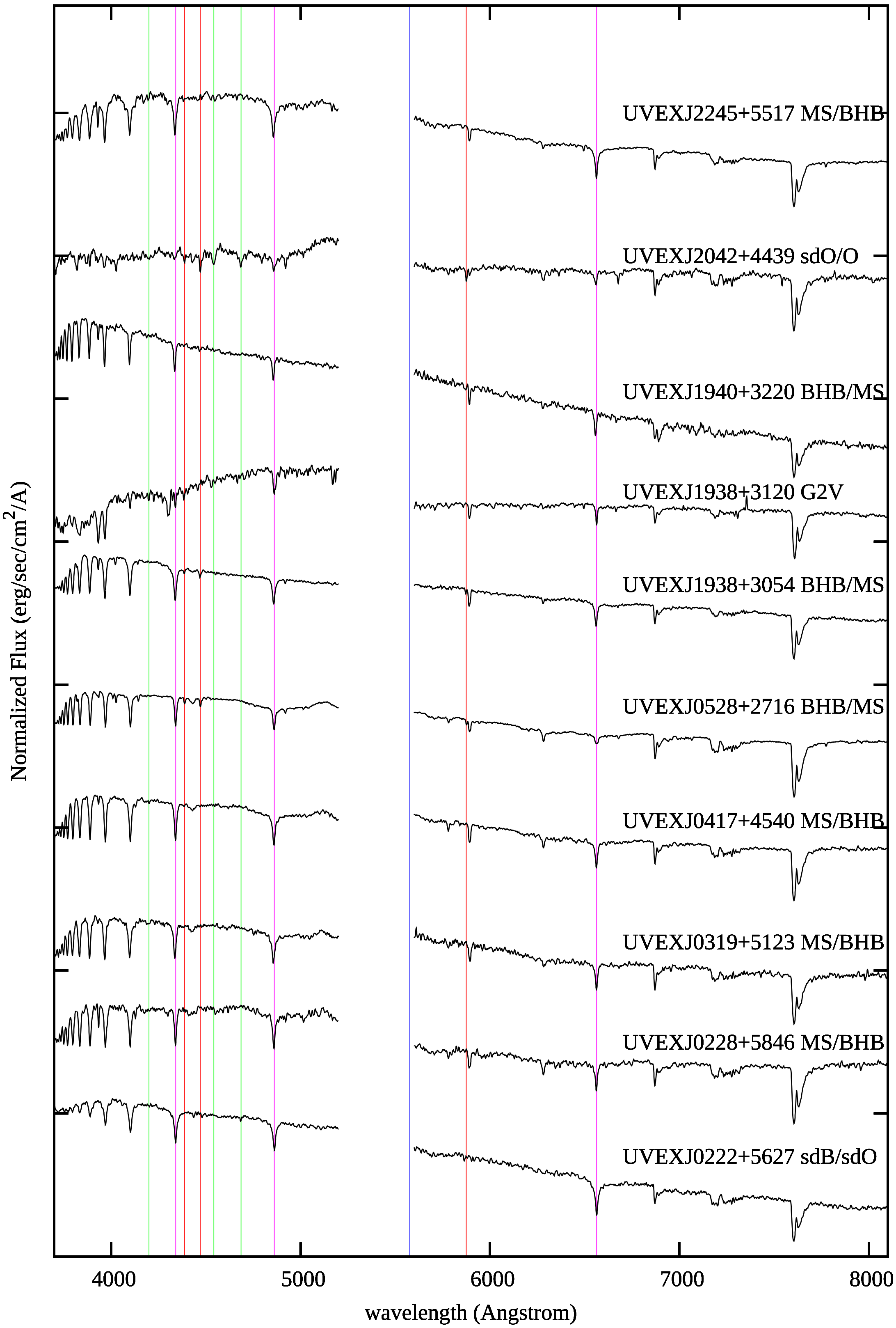

Figure A7. The UV-excess spectra classified as MS/BHB stars, probably sdB/sdO/O type stars and 1 G-type star. The pink, red and green lines indicate the position of hydrogen, HeI and HeII respectively. The blue line is a skyline in the Hectospec spectra.

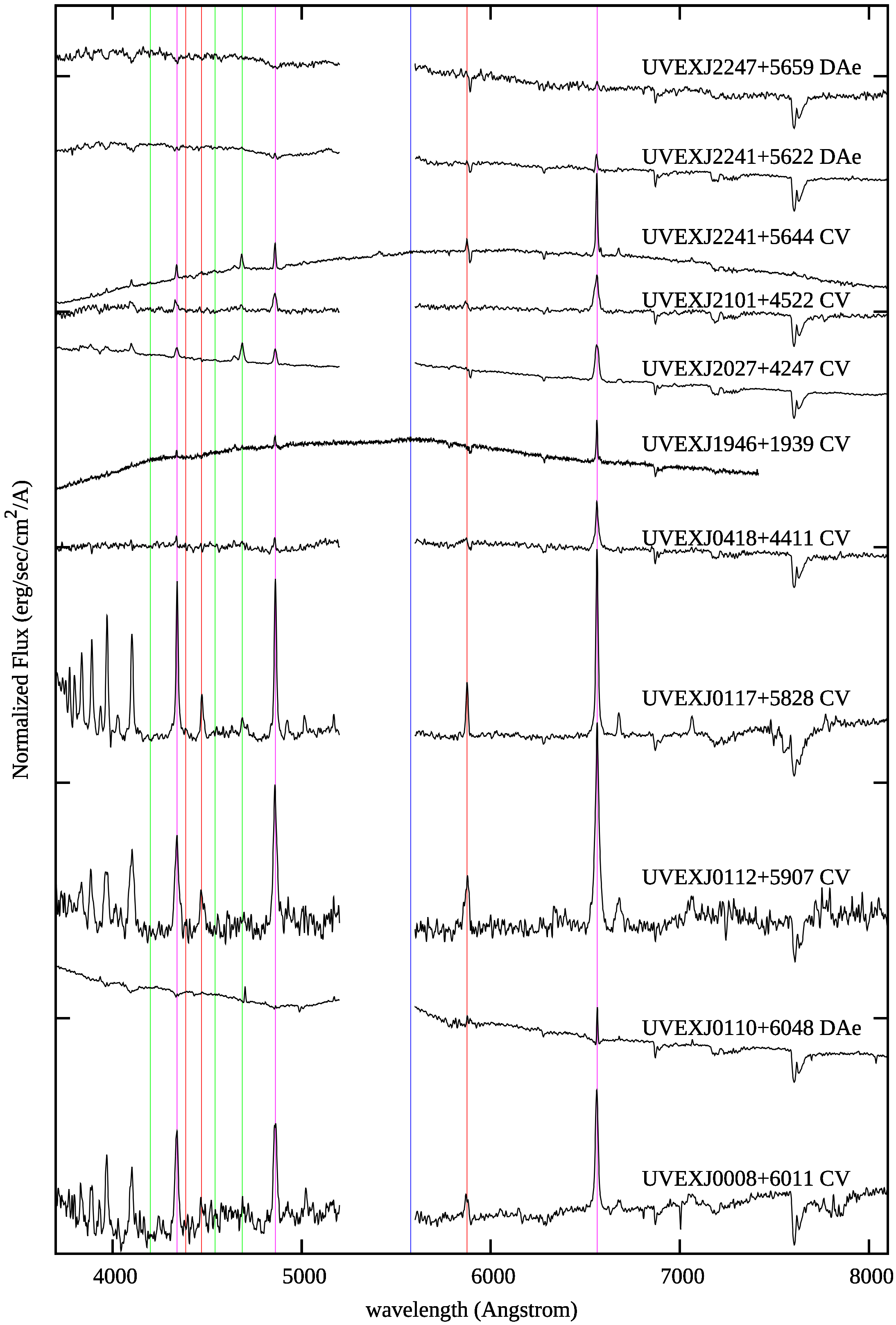

Figure A8. All UV-excess spectra classified as Cataclysmic Variables and DAe white dwarfs. The pink, red and green lines indicate the position of hydrogen, HeI and HeII respectively. The blue line is a skyline in the Hectospec spectra.

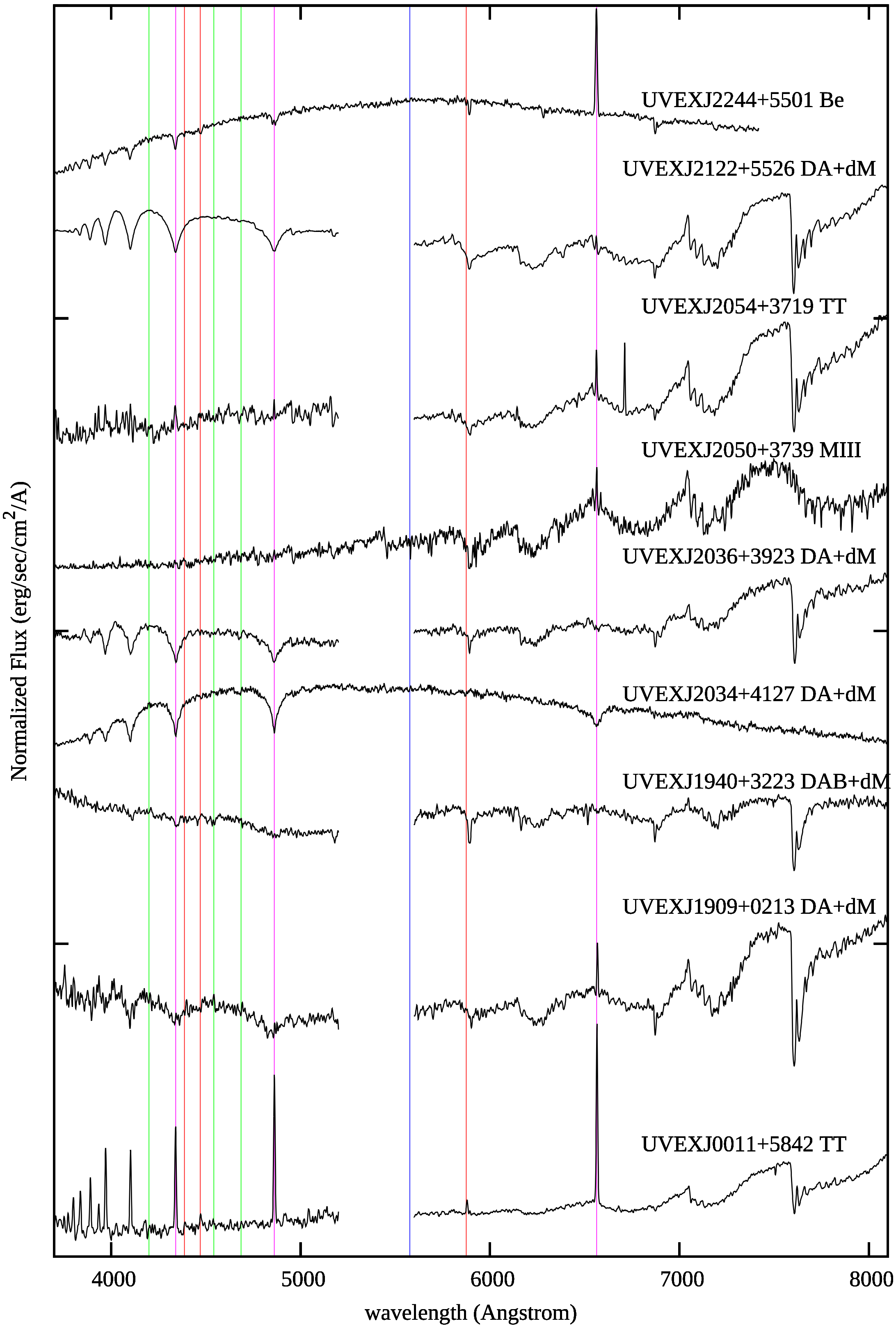

Figure A9. The UV-excess spectra classified as DA+dM systems, T Tauri stars, Be star and 1 M5III giant. The pink, red and green lines indicate the position of hydrogen, HeI and HeII respectively. The blue line is a skyline in the Hectospec spectra.

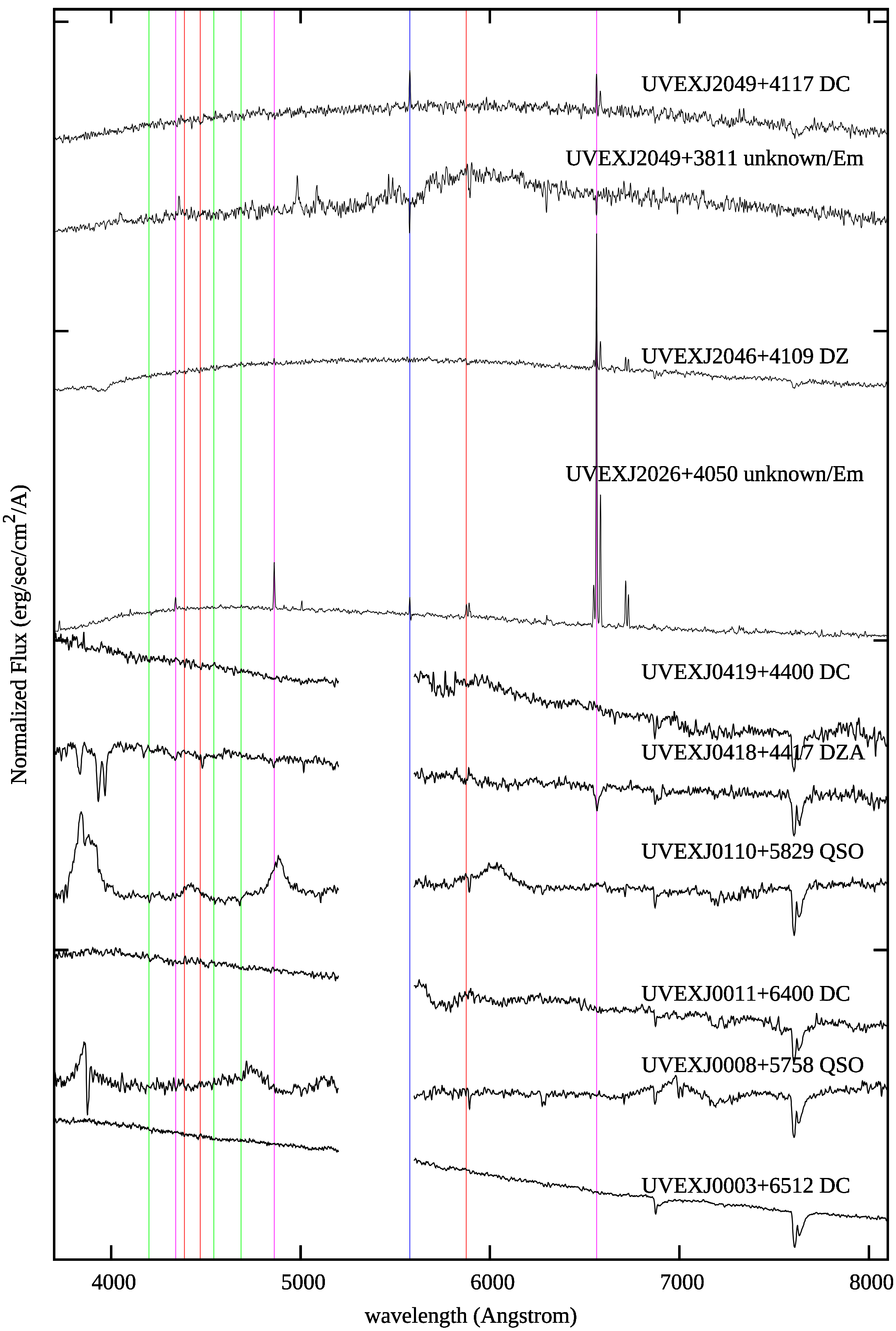

Figure A10. UV-excess spectra classified as DC and DZ white dwarfs, QSOs and 2 unknown sources. Note that the emission lines of the 2 unknown sources, also present in the sky offset spectra, are due to diffuse emission in the field. The pink, red and green lines indicate the position of hydrogen, HeI and HeII respectively. The blue line is a skyline in the Hectospec spectra.

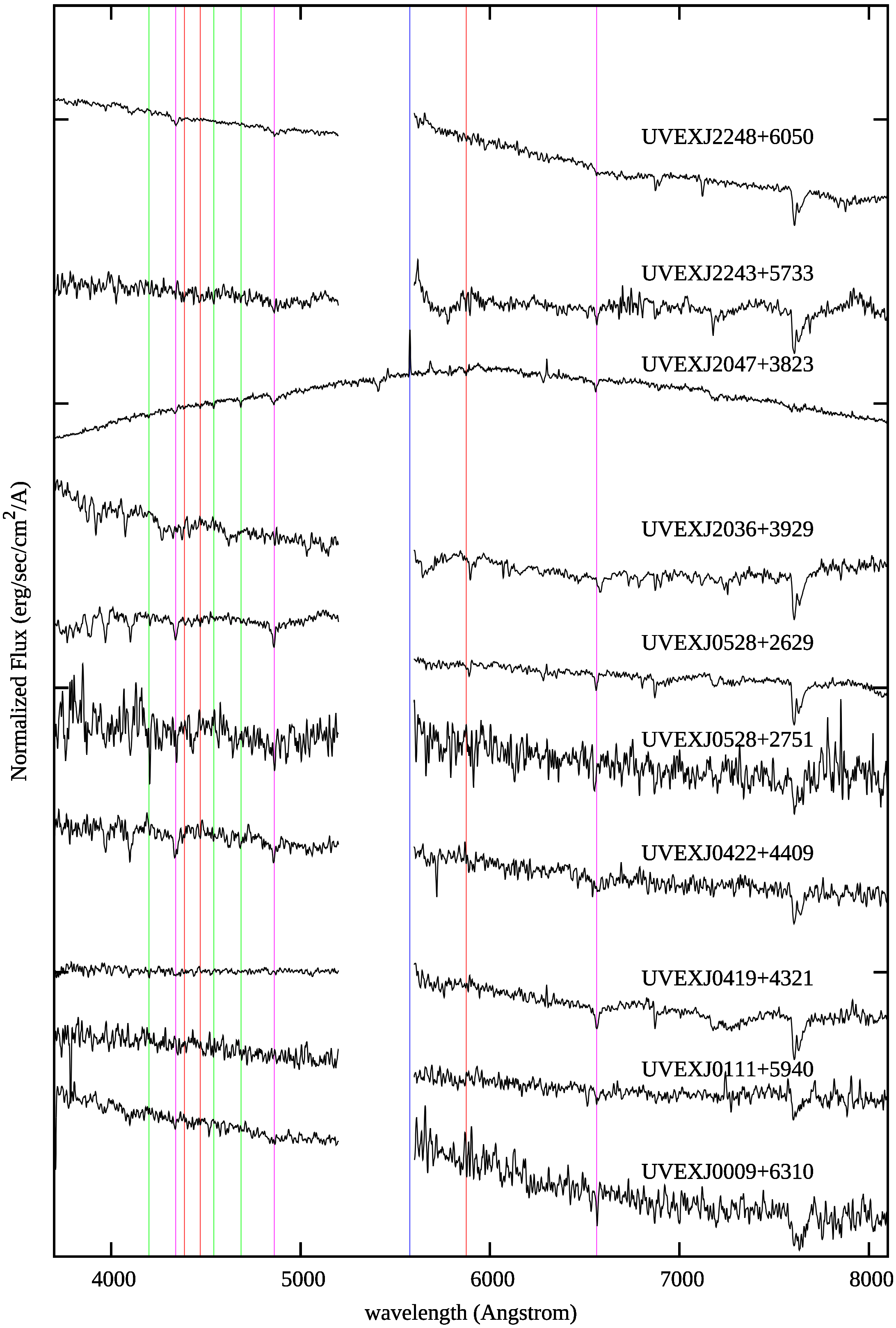

Figure A11. UV-excess spectra classified as "Noisy". The pink, red and green lines indicate the position of hydrogen, HeI and HeII respectively. The blue line is a skyline in the Hectospec spectra.

Table AA1. Classifications of the UV-excess spectra.

No	Name	l	b	Field	Selection	g	$(U-g)$	$(g-r)$	(HeI)	$(r-i)$	$(r-H\alpha)$	Run	Classification	Fit
1	UVEXJ000016.27+603246.3	116.67893	-1.70286	9	519	16.761	-0.687	0.212	16.534	-0.433	0.371	WHT2010dec12	sdB	34.4/6.0/−2.8
2	UVEXJ000218.56+623649.3	117.31640	+0.27881	6	1543	18.073	-0.852	0.017	18.282	0.001	0.281	WHT2010dec12	DB	16.0
3	UVEXJ000310.20+633430.2	117.59252	+1.20480	8	519	17.387	-0.796	0.07	17.492	-0.037	0.531	WHT2010dec12	DBA	14.0
4	UVEXJ000313.11+651248.1	117.90273	+2.81352	22	1543	17.619	-0.584	0.149	17.516	0.263	0.177	WHT2008oct03	DC	
5	UVEXJ000355.86+632833.2	117.65757	+1.09168	19	519	16.380	-0.583	0.149	16.232	0.077	0.062	Fast2009feb03	DAB	
6	UVEXJ000843.60+601154.7	117.64423	-2.23399	40	515	19.837	-0.485	1.179	18.649	0.879	0.829	WHT2010dec13	CV	18/−50
7	UVEXJ000848.64+575832.7	117.28742	-4.42807	48	515	19.494	-0.092	0.869	18.743	0.734	0.360	WHT2010dec12	QSO	(z=1.48)
8	UVEXJ000919.43+583729.7	117.46085	-3.79876	52	519	18.162	-0.217	0.729	17.597	0.563	0.238	WHT2010dec12	DAB	
9	UVEXJ000945.33+631032.4	118.24989	+0.68346	51	1543	17.983	-0.962	-0.041	17.967	0.074	0.185	WHT2010dec14	noisy	O5V,0.3
10	UVEXJ001032.27+625050.0	118.28513	+0.34507	62	514	16.427	0.108	0.555	15.901	0.429	0.233	Fast2011nov30	He-sdO	
11	UVEXJ001101.26+640013.7	118.52021	+1.47880	55	1543	19.564	-0.476	0.306	19.360	0.349	0.189	WHT2009sep21	DC	
12	UVEXJ001102.23+584232.3	117.69466	-3.75135	52	515	19.710	-0.151	1.548	18.743	1.932	1.381	WHT2010dec10	TTauri(M4V)	6/−80
13	UVEXJ011037.91+582928.1	125.44465	-4.28694	404	515	19.518	-0.158	0.697	19.003	0.576	0.403	WHT2009sep21	QSO	(z=2.16)
14	UVEXJ011053.07+604830.9	125.30232	-1.97363	410	1543	17.026	-0.895	-0.006	17.162	0.128	0.168	WHT2010dec13	DAe	
15	UVEXJ011102.67+594020.8	125.40836	-3.10500	389	1543	18.839	-0.561	0.143	18.672	-0.104	0.218	WHT2009sep22	noisy	
16	UVEXJ011245.47+590757.3	125.66906	-3.62581	405	519	18.306	-0.272	0.598	17.681	0.298	0.668	WHT2009sep23	CV	25/−150
17	UVEXJ011311.87+581902.3	125.79454	-4.43345	402	1028	18.130	0.052	0.153	18.052	0.095	-0.125	WHT2009sep21	DA	10.0
18	UVEXJ011712.36+582804.4	126.30500	-4.23500	436	515	19.143	-0.798	0.906	0.000	0.857	0.892	WHT2010dec12	CV	14/−60
19	UVEXJ011754.90+581815.4	126.41435	-4.38833	436	1028	17.736	-0.31	-0.031	0.000	0.005	-0.231	WHT2010dec14	DA	11.9/8.3
20	UVEXJ012015.68+584318.2	126.67481	-3.94040	437	1028	18.838	-0.761	0.039	0.000	0.119	0.094	WHT2010dec13	DA	36.9/8.1
21	UVEXJ012219.81+611229.9	126.64407	-1.44059	463	1543	17.509	-0.318	-0.017	0.000	-0.015	-0.136	WHT2009sep25	DA	12.8/8.1
22	UVEXJ012359.82+672223.1	126.06509	+4.69962	457	1543	18.659	-0.598	0.175	0.000	0.050	0.108	WHT2009sep25	DA	57.0
23	UVEXJ020201.82+564744.8	132.52194	-4.75581	679	1543	19.230	-0.948	-0.049	19.372	no data	no data	WHT2009sep23	DA	65.0
24	UVEXJ020201.85+564342.3	132.54031	-4.82064	679	519	15.238	-0.667	-0.019	15.319	no data	no data	WHT2009sep25	sdB	27.5/5.5/−2.8
25	UVEXJ022113.52+564810.7	135.02814	-3.94521	784	519	17.267	-0.833	0.375	16.989	-0.026	0.162	WHT2009sep24	He-sdO	44.0/5.5/1.4
26	UVEXJ022135.47+564436.6	135.09570	-3.98401	784	519	18.582	-0.318	0.383	18.200	-0.080	-0.084	WHT2009sep22	DA	10.1/8.0
27	UVEXJ022151.40+563815.7	135.16636	-4.07093	784	1543	19.606	-0.892	0.199	19.379	-0.327	0.199	WHT2010dec13	DA	28.6/8.2
28	UVEXJ022241.76+562702.2	135.33986	-4.20672	800	518	17.895	-0.314	0.291	17.729	0.156	0.115	WHT2009sep22	noisy	B3V,0.4
29	UVEXJ022510.84+580156.6	135.10038	-2.60741	814	1543	17.920	-0.118	-0.49	0.000	-0.030	-0.223	WHT2010dec12	DA	13.1/8.0
30	UVEXJ022615.13+581710.2	135.14207	-2.31994	814	1028	18.970	-0.251	-0.167	0.000	0.108	-0.042	WHT2010dec12	DA	9.8/8.5
31	UVEXJ022815.18+584640.8	135.20774	-1.76697	820	514	18.200	0.106	0.959	0.000	0.525	0.213	WHT2010dec12	MS/BHB	14.2/3.8/F0V,0.1
32	UVEXJ023044.92+563622.6	136.32179	-3.66150	838	1543	18.789	-0.772	-0.118	0.000	-0.001	0.062	WHT2010dec13	DA	30.0/8.2
33	UVEXJ031943.45+512309.0	145.11863	-4.98344	1153	518	17.368	0.151	0.478	16.904	0.306	0.169	WHT2010dec14	MS/BHB	15.8/4.3/F0V,0.0
34	UVEXJ032737.64+530231.1	145.21912	-2.93464	1206	1028	17.555	-0.415	-0.006	17.521	-0.010	-0.078	WHT2010dec14	DA	18.5/8.1
35	UVEXJ032807.05+525737.2	145.32615	-2.96070	1230	1543	18.372	-0.558	0.06	18.432	-0.147	0.044	WHT2009sep21	DA	23.9/7.8
36	UVEXJ032855.25+503529.8	146.76969	-4.84547	1224	519	14.202	-0.558	0.127	14.085	-0.015	0.109	WHT2009sep25	sdB	28.5/5.5/−2.5
37	UVEXJ032908.01+524400.6	145.58117	-3.06136	1222	1543	18.484	-0.503	0.072	18.370	0.055	-0.067	WHT2009sep21	DA	22.3/7.8
38	UVEXJ032910.60+524426.3	145.58251	-3.05178	1222	1543	17.068	-0.417	-0.034	17.027	-0.067	-0.123	WHT2009sep21	DA	12.8/8.1
39	UVEXJ033118.06+530351.3	145.66179	-2.60337	1230	1543	16.975	-0.505	-0.055	16.919	-0.198	-0.196	WHT2009sep22	DA	17.1/8.1
40	UVEXJ041045.70+461137.1	154.95071	-3.91735	1567	519	17.596	-0.307	0.098	17.447	-0.038	-0.135	WHT2010dec14	DA	14.5/7.6
41	UVEXJ041053.99+450706.5	155.70394	-4.68702	1553	1543	19.860	-0.199	0.162	0.000	0.319	-0.375	WHT2009sep22	DA	16.1/7.8
42	UVEXJ041359.37+455151.2	155.58583	-3.77300	1585	1028	17.494	-0.221	0.078	0.000	-0.135	-0.130	WHT2009sep21	DA	12.3/8.1
43	UVEXJ041733.05+452524.4	156.34147	-3.65845	1629	1543	18.910	-0.539	0.029	18.876	0.136	0.005	WHT2009sep21	DA	22.6/8.0
44	UVEXJ041745.78+454049.8	156.18824	-3.44853	1629	518	17.322	0.193	0.535	16.886	0.443	0.172	WHT2010dec12	MS/BHB	13.4/3.9/F0V,0.0
45	UVEXJ041824.24+441152.2	157.30940	-4.42838	1635	519	18.132	-0.112	0.599	17.640	0.472	0.473	WHT2010dec13	CV	20/−20
46	UVEXJ041840.30+441714.1	157.28080	-4.33102	1635	1028	19.870	-0.458	0.162	19.820	-0.038	-0.017	WHT2009sep23	DZA	
47	UVEXJ041902.55+434307.1	157.72889	-4.68909	1628	1543	17.829	-0.377	-0.021	17.838	0.014	-0.123	WHT2010dec14	DA	17.4/8.0
48	UVEXJ041914.11+432147.8	158.00454	-4.91725	1628	1543	17.167	-0.266	0.23	16.925	0.187	0.017	WHT2010dec14	noisy	B8V,0.5
49	UVEXJ041926.84+440058.4	157.57106	-4.42618	1635	1543	19.073	-0.611	0.13	18.986	-0.007	0.158	WHT2010dec12	DC	
50	UVEXJ042023.52+473534.8	155.16783	-1.76858	1659	1543	16.055	-0.998	-0.057	16.204	-0.013	0.128	WHT2009sep25/F	DAB	
51	UVEXJ042110.67+440945.6	157.68835	-4.10319	1661	1028	19.035	-0.39	0.099	18.848	0.041	-0.163	WHT2009sep23	DA	20.5/7.8
52	UVEXJ042125.70+465115.4	155.81393	-2.16822	1672	514	18.107	0.48	0.877	17.451	0.637	0.287	WHT2009sep21	sdB+F	
53	UVEXJ042223.30+440945.3	157.84196	-3.94941	1661	1543	19.397	-0.443	0.239	19.134	0.240	-0.052	WHT2009sep24	noisy	
54	UVEXJ052823.37+275159.7	178.86901	-3.77121	2465	519	19.680	-0.362	0.313	0.000	no data	no data	WHT2010dec13	noisy	B3V,0.4
55	UVEXJ052825.82+320859.5	175.30149	-1.39485	2458	1543	18.501	-0.32	0.093	0.000	no data	no data	WHT2010dec12	DA	9.9/8.3
56	UVEXJ052835.30+271650.0	179.38341	-4.05755	2454	515	14.499	0.155	0.5	0.000	no data	no data	WHT2010dec12	BHB/MS	17.3/3.7/B3V,0.5
57	UVEXJ052847.75+322330.3	175.14281	-1.19658	2458	1028	18.876	-0.06	0.082	0.000	no data	no data	WHT2010dec13	DA	12.9/7.9
58	UVEXJ052851.01+262946.3	180.07233	-4.44047	2467	519	18.980	0.007	0.578	0.000	no data	no data	WHT2010dec13	noisy	B3V,0.6
59	UVEXJ185740.07+075557.3	40.70227	+2.23345	4346	1028	18.934	-0.312	0.168	18.817	0.307	0.058	Hect2006may02	DA	
60	UVEXJ190812.07+164029.2	49.66841	+3.92988	4556	1028	17.292	-0.619	0.051	17.157	-0.102	-0.074	WHT2010dec14	DA	17.0
61	UVEXJ190912.34+021342.8	36.94523	-2.93167	4580	519	18.764	-0.218	0.867	18.220	1.290	0.643	WHT2010dec13	DA+dM	DA+M2Ve
62	UVEXJ193809.18+305401.5	65.47669	+4.56471	5150	519	17.038	-0.297	0.197	0.000	0.015	0.112	WHT2009sep23	BHB/MS	18.9/4.5/B3V,0.4
63	UVEXJ193813.83+313708.1	66.11524	+4.89870	5129	1543	17.373	-0.996	-0.074	0.000	-0.101	0.035	WHT2009sep23	sdO	50.4/5.7/−1.47
64	UVEXJ193847.06+312024.2	65.92808	+4.66012	5160	519	19.481	-0.743	0.161	19.467	0.104	0.088	WHT2009sep25	G0V-G2V	G2V,0.3
65	UVEXJ193951.69+302600.7	65.24726	+4.01643	5182	519	17.358	-0.502	0.199	17.201	0.118	0.131	WHT2009sep24	sdB	27.8/4.6/−1.5
66	UVEXJ194028.01+322039.8	66.98290	+4.83719	5186	1543	18.638	-0.349	0.179	18.442	0.084	0.236	WHT2009sep24	BHB/MS	16.0/3.1/B0V,0.4
67	UVEXJ194059.93+322347.8	67.08369	+4.76468	5186	515	19.237	-0.725	0.67	18.687	0.820	0.439	WHT2010dec13	DAB+dM	DAB+M1V
68	UVEXJ194135.69+321222.0	66.97892	+4.56159	5186	1028	18.892	-0.82	0.065	18.891	0.190	0.144	WHT2009sep23	sdB	31.0/6.0/−1.9
69	UVEXJ194633.12+193926.4	56.64074	-2.64941	5284	519	15.135	-0.461	0.331	14.809	0.282	0.355	Fast2011jun09	CV	
70	UVEXJ202249.99+412423.1	79.15873	+2.42925	5853	1028	19.718	-0.248	0.049	19.544	-0.154	-0.520	WHT2009sep24	DA	15.6/8.2
71	UVEXJ202255.55+412504.9	79.17820	+2.42162	5853	1028	18.766	-0.307	-0.003	18.651	-0.080	-0.259	WHT2009sep24	DA	16.3/8.0
72	UVEXJ202350.92+423826.0	80.28021	+2.98039	5875	1543	18.641	-0.824	-0.133	18.781	-0.178	0.173	WHT2010dec12	DA	25.3/8.5
73	UVEXJ202439.91+400630.7	78.29391	+1.40076	5892	1031	19.905	-0.749	-0.178	20.005	-0.252	-0.080	WHT2009sep24	DA	24.0
74	UVEXJ202457.34+410804.1	79.16473	+1.94658	5879	1028	19.768	-0.433	-0.071	19.824	-0.117	-0.030	WHT2009sep24	DA	22.0
75	UVEXJ202501.86+411626.0	79.28692	+2.01532	5916	1028	18.627	-0.305	-0.005	18.703	-0.113	-0.166	WHT2009sep25	DA	14.8/8.2

Table AA2. Table AA1 continued

No	Name	l	b	Field	Selection	g	$(U-g)$	$(g-r)$	(HeI)	$(r-i)$	$(r-H\alpha)$	Run	Classification	Fit
76	UVEXJ202557.21+400949.2	78.48112	+1.23151	5892	1028	18.429	-0.735	-0.204	18.469	-0.164	-0.522	WHT2009sep24	DA	30.0
77	UVEXJ202630.19+405024.1	79.09318	+1.53808	5902	1028	19.880	-0.182	0.145	19.864	-0.020	0.378	Hect2005oct23	unknown/Em	
78	UVEXJ202659.21+411644.1	79.50370	+1.71848	5916	1028	17.092	-0.703	-0.083	17.077	0.073	0.047	Hect2005oct22	DA	
79	UVEXJ202712.06+424720.1	80.75706	+2.56286	5947	519	16.079	-0.385	0.33	15.864	0.176	0.464	WHT2009sep21	CV(novalike)	24/–21
80	UVEXJ202744.63+405044.5	79.23419	+1.35043	5939	1543	19.134	-0.814	-0.084	19.363	-0.152	0.041	Hect2005oct22	DB	
81	UVEXJ202800.47+405620.0	79.33903	+1.36420	5939	1028	16.167	-0.754	-0.157	16.258	-0.147	-0.148	WHT2009sep21	DA	20.0
82	UVEXJ202807.55+411357.7	79.59074	+1.51750	5951	1543	18.939	-0.662	-0.082	19.056	0.045	-0.159	Hect2005oct22	DA	
83	UVEXJ202922.26+412815.9	79.92088	+1.46732	5951	1029	20.161	-0.309	0.081	19.946	-0.035	-0.017	Hect2005oct22	DA	
84	UVEXJ203039.82+413252.3	80.12526	+1.31662	5985	1543	19.436	-0.373	-0.04	19.386	-0.104	-0.105	Hect2004jun10	DA	
85	UVEXJ203238.52+411339.4	80.08644	+0.82801	6010	1543	19.295	-0.775	-0.151	19.486	-0.101	-0.127	Hect2004jun10	DA	
86	UVEXJ203352.73+405647.0	79.99913	+0.47336	6010	1028	18.461	-0.978	-0.199	18.573	-0.202	0.031	Hect2006oct10	DA	
87	UVEXJ203411.72+411020.3	80.21601	+0.56034	6010	1543	20.428	-0.5	-0.015	20.333	0.212	-0.395	Hect2006oct10	DA	
88	UVEXJ203413.57+404702.9	79.90816	+0.32382	6035	1029	19.615	-0.309	0.034	19.681	-0.095	-0.214	Hect2005jul01	DA	
89	UVEXJ203421.28+404827.4	79.94151	+0.31834	6035	1028	20.521	-0.288	0.157	20.380	-0.084	-0.182	Hect2005jul02	DA	
90	UVEXJ203455.77+412735.1	80.52884	+0.62177	6046	1028	20.884	-0.457	0.71	0.000	0.109	-0.131	Hect2006oct10	DA+dM	
91	UVEXJ203519.00+403408.9	79.85970	+0.02950	6035	1029	19.580	-0.511	0.001	19.587	-0.103	-0.244	Hect2006oct10	DA	
92	UVEXJ203614.30+392309.8	79.02005	-0.82249	6036	1029	19.776	-0.584	0.194	19.635	0.821	0.326	WHT2009sep25	DA+dM	DA+M3V
93	UVEXJ203656.54+392934.9	79.18734	-0.86650	6066	1543	18.882	-1.144	-0.178	19.100	-0.219	0.025	WHT2009sep23	noisy/WD?	
94	UVEXJ203739.63+413216.3	80.89908	+0.26049	6080	1028	19.645	-0.376	-0.002	19.779	0.162	-0.198	WHT2009sep23/H	DA	17.0
95	UVEXJ204101.05+414327.9	81.42907	-0.12343	6112	1543	19.682	-0.299	0.289	19.410	0.154	0.109	Hect2004jun19	DA	
96	UVEXJ204210.22+443928.7	83.87361	+1.51222	6107	519	18.738	0.002	0.891	18.055	0.712	0.513	WHT2010dec13	sdO?	B0V,0.9
97	UVEXJ204649.51+410906.2	81.65384	-1.33263	6186	1543	20.158	-0.323	0.178	20.186	0.165	0.239	Hect2004jun25	DZ	
98	UVEXJ204710.61+413133.5	81.98697	-1.14960	6166	1543	18.945	-1.032	-0.137	19.311	-0.115	-0.031	Hect2004jun26	DA	
99	UVEXJ204751.27+442920.1	84.37091	+0.61442	6196	1028	19.960	-0.503	-0.044	20.165	0.242	0.020	Hect2004nov20	DA	
100	UVEXJ204758.19+382323.2	79.63810	-3.23534	6181	519	19.054	-0.239	0.639	18.605	0.454	0.267	Hect2004nov20	noisy	
101	UVEXJ204923.48+381139.0	79.66150	-3.57521	6211	1542	18.891	-0.126	0.497	18.512	0.266	0.463	Hect2004nov12	unknown/Em	
102	UVEXJ204925.78+411725.6	82.06990	-1.62608	6217	1543	20.809	0.06	0.573	20.196	0.533	0.189	Hect2004jun25	DC	
103	UVEXJ204932.62+374048.2	79.28056	-3.92266	6201	1028	18.577	-0.535	-0.027	18.519	0.031	-0.194	Hect2004nov12	DA	
104	UVEXJ204945.83+382057.2	79.82825	-3.53410	6211	1543	19.749	-0.374	0.035	19.527	-0.371	0.297	Hect2004nov12	DA	
105	UVEXJ204957.75+401637.9	81.34841	-2.34506	6226	519	15.741	-0.67	0.334	15.485	0.206	0.179	WHT2010dec13	He-sdO	45.9/6.1/1.4
106	UVEXJ205037.81+424618.9	83.35761	-0.85988	6220	1543	15.758	-0.571	-0.042	15.730	-0.072	-0.144	WHT2008oct05	DA	17.0
107	UVEXJ205039.07+373958.4	79.40858	-4.10129	6218	1031	21.119	-0.535	0.283	18.981	0.098	2.248	Hect2004nov12	M5III	M5III
108	UVEXJ205056.87+380710.6	79.79745	-3.85943	6231	519	20.404	-0.285	0.588	20.150	0.369	0.355	Hect2004nov20	DAB/DA	
109	UVEXJ205148.13+442408.8	84.75023	+0.01441	6219	1028	17.716	-0.888	-0.098	17.874	-0.120	0.015	WHT2009sep22	DA	26.0
110	UVEXJ205449.65+371953.2	79.67935	-4.95297	6267	519	18.396	-0.471	0.606	17.971	1.848	0.956	WHT2010dec13	TTauri(M5V)	4/–9
111	UVEXJ210037.77+501029.0	90.11721	+2.61574	6323	1543	16.542	-0.735	-0.154	16.626	-0.283	-0.092	WHT2010dec14	DA	20.9/7.9
112	UVEXJ210127.26+452247.2	86.60349	-0.65097	6355	519	18.185	0.044	0.597	0.000	0.571	0.562	WHT2009sep21	CV	28/–22
113	UVEXJ210248.44+475058.9	88.60784	+0.81096	6341	1543	18.300	-0.421	-0.013	18.176	no data	no data	WHT2010dec12	DA	13.3/8.1
114	UVEXJ210454.41+460041.9	87.47634	-0.68123	6365	1543	18.743	-0.837	-0.037	18.914	-0.177	0.221	WHT2010dec12	DB	16.0
115	UVEXJ211718.18+550638.7	95.46871	+4.09795	6496	1543	17.342	-0.597	-0.078	17.335	-0.062	-0.087	WHT2009sep22	DA	22.0
116	UVEXJ212257.82+552609.0	96.26868	+3.75358	6555	519	15.057	-0.13	0.455	14.822	1.318	0.512	WHT2009sep22	DA+dM	DA+M1V
117	UVEXJ212409.05+555521.4	96.73083	+3.98237	6561	1028	17.952	-0.245	0.046	17.719	no data	no data	WHT2009sep21	DA	12.0
118	UVEXJ212705.33+541058.2	95.81804	+2.44184	6597	1543	18.929	-0.799	-0.042	19.150	-0.117	0.147	WHT2010dec13	DB	18.0
119	UVEXJ212852.14+542048.4	96.11948	+2.38077	6603	1028	18.126	-0.395	-0.047	18.030	0.003	-0.162	WHT2010dec13	DA	13.9/8.2
120	UVEXJ222940.17+610700.7	106.64583	+2.81053	7084	1543	17.489	-0.789	-0.111	17.553	0.001	-0.022	WHT2010dec14	DA	22.3/8.0
121	UVEXJ223634.77+591907.8	106.47749	+0.82554	7139	1028	17.647	-0.724	-0.081	17.645	-0.018	-0.023	WHT2010dec14	DA	28.7/8.0
122	UVEXJ223811.54+603759.9	107.29952	+1.87109	7155	1543	18.533	-0.65	0.14	18.350	0.003	-0.166	WHT2010dec13	DA	12.6/8.1
123	UVEXJ223941.98+585729.1	106.65014	+0.31521	7153	515	16.020	-0.289	0.496	15.594	0.297	0.228	WHT2010dec13	He-sdO	47.7/5.0/–0.74
124	UVEXJ224010.23+555950.6	105.27455	-2.30746	7171	1028	17.741	-0.651	-0.086	17.796	-0.028	-0.061	WHT2010dec10	DA	20.0/3.0
125	UVEXJ224112.21+564419.1	105.75676	-1.72636	7179	518	18.978	-0.078	0.56	18.634	0.428	0.545	Hect2005jul05	CV(magnetic)	
126	UVEXJ224145.94+562230.0	105.65079	-2.08275	7171	514	17.981	-0.221	0.561	17.569	0.385	0.342	WHT2010dec13	DAe	
127	UVEXJ224324.38+573324.0	106.40874	-1.14878	7173	1543	19.666	-0.492	0.381	19.274	0.215	0.006	WHT2010dec13	noisy	
128	UVEXJ224435.05+550104.9	105.35839	-3.46612	7188	514	14.917	-0.039	0.388	14.618	0.308	0.495	Fast2009nov21	Be	
129	UVEXJ224521.39+551705.3	105.58100	-3.28184	7197	1028	19.632	-0.661	-0.033	19.605	-0.176	-0.168	WHT2010dec14	MS/BHB	14.9/4.7/F0V,0.1
130	UVEXJ224610.82+611450.3	108.44539	+1.94933	7189	1028	17.974	-0.456	-0.088	18.009	-0.005	-0.059	WHT2010dec14	DA	20.0/8.1
131	UVEXJ224721.36+565937.4	106.61932	-1.89546	7203	518	17.736	-0.114	0.468	17.356	0.399	0.257	WHT2010dec14	DAe	
132	UVEXJ224835.69+605057.8	108.52252	+1.46171	7206	1028	17.446	-0.779	0.047	17.375	0.008	0.066	WHT2010dec10	noisy	O5V,0.4